

VILNIUS UNIVERSITY
CENTER FOR PHYSICAL SCIENCES AND TECHNOLOGY

RENATA ŽENOVIENĖ

CHEMICAL COMPOSITION STUDY OF GALACTIC STELLAR
SUBSTRUCTURES

Summary of Doctoral Dissertation
Physical Sciences, Physics (02 P)

Vilnius, 2015

Doctoral Dissertation was completed during 2010–2015 at Institute of Theoretical Physics and Astronomy of Vilnius University.

Scientific supervisor – Dr. Habil. Gražina Tautvaišienė (Vilnius University, Institute of Theoretical Physics and Astronomy, Physical sciences, Physics – 02 P).

Doctoral Dissertation will be defended at the Council of Physical sciences of Vilnius University:

Chairman – Dr. Habil. Kazimieras Zdanavičius (Vilnius University, Institute of Theoretical Physics and Astronomy, Physical Sciences – 02 P).

Members:

Prof. Dr. Paulius Miškinis (Vilnius Gediminas Technical University, Physical Sciences – 02 P),

Dr. Algirdas Stasius Kazlauskas (Vilnius University, Physical Sciences – 02 P),

Dr. Stanislava Bartašiutė (Vilnius University, Physical Sciences – 02 P),

Doc. Dr. Andreas Korn (Uppsala University, Physical Sciences – 02 P).

Doctoral Dissertation will be defended at the public meeting of the Council of Physical sciences of Vilnius University held at Vilnius University Institute of Theoretical Physics and Astronomy at 2:00 p.m. on 6 May, 2015.

Address: A. Goštauto St. 12, 01108 Vilnius, Lithuania. The Thesis is available at the libraries of Vilnius University and Center For Physical Sciences and Technology, and on the web page of Vilnius University: www.vu.lt/lt/naujienos/ivykiu-kalendorius.

VILNIAUS UNIVERSITETAS
FIZINIŲ IR TECHNOLOGIJOS MOKSLŲ CENTRAS

RENATA ŽENOVIENĖ

CHEMINĖS SUDĖTIES TYRIMAS GALAKTIKOS ŽVAIGŽDŽIŲ
SUBSTRUKTŪROSE

Daktaro disertacijos santrauka
Fiziniai mokslai, fizika (02 P)

Vilnius, 2015

Daktaro disertacija rengta 2010–2015 metais Vilniaus universiteto Teorinės fizikos ir astronomijos institute.

Mokslinis vadovas – habil. dr. Gražina Tautvaišienė (Vilniaus universiteto Teorinės fizikos ir astronomijos institutas, fiziniai mokslai, fizika – 02 P).

Disertacija ginama Vilniaus universiteto Fizikos mokslo (02P) krypties taryboje.

Pirmininkas – habil. dr. Kazimieras Zdanavičius (Vilniaus universiteto Teorinės fizikos ir astronomijos institutas, fiziniai mokslai, fizika – 02 P).

Nariai:

Prof. dr. Paulius Miškinis (Vilniaus Gedimino technikos universitetas, fiziniai mokslai, fizika – 02 P),

Dr. Algirdas Stasius Kazlauskas (Vilniaus universitetas, fiziniai mokslai, fizika – 02 P),

Dr. Stanislava Bartašiūtė (Vilniaus universitetas, fiziniai mokslai, fizika – 02 P),

Doc. dr. Andreas Korn (Upsalos universitetas, fiziniai mokslai, fizika – 02 P).

Disertacija bus ginama viešame Fizikos mokslo krypties tarybos posėdyje 2015 m. gegužės mėn. 06 d. 14 val. Vilniaus universiteto Teorinės fizikos ir astronomijos institute.

Adresas: A. Goštauto g. 12, 01108 Vilnius, Lietuva.

Disertaciją galima peržiūrėti Vilniaus universiteto, Fizinių ir technologijos mokslo centro bibliotekose ir VU interneto svetainėje adresu:

www.vu.lt/lt/naujienos/ivykiu-kalendorius.

Contents

| | |
|---|-----------|
| Introduction | 7 |
| Aims of the study | 8 |
| Tasks of the study | 8 |
| Scientific novelty | 9 |
| Results and statements presented for defense | 9 |
| Personal contribution | 10 |
| Publications on the subject of the dissertation | 10 |
| Presentations at the international conferences | 12 |
| Thesis outline | 13 |
| 1 Kinematic groups of stars | 15 |
| 1.1 Kinematic stellar groups in the solar neighbourhood | 15 |
| 1.2 Kinematic Group 1 and Group 2 of the Geneva-Copenhagen Survey . | 16 |
| 2 Observations and analysis | 21 |
| 2.1 Observations | 21 |
| 2.2 Differential analysis | 21 |
| 2.2.1 Software packages and model atmospheres | 21 |
| 2.2.2 Atomic data | 22 |
| 2.2.3 Synthetic spectra | 23 |
| 2.2.4 Determination of main atmospheric parameters | 25 |
| 2.2.5 Uncertainties | 25 |
| 3 Results and discussion | 27 |
| 3.1 Main atmospheric parameters | 27 |
| 3.2 Comparison with previous studies | 27 |
| 3.3 The detailed elemental abundances | 31 |
| 3.4 Age distribution | 36 |
| 3.5 Comparison with kinematic streams | 40 |
| 3.6 Origin | 42 |
| 4 Main results and conclusions | 45 |
| Bibliography | 47 |
| Santrauka | 52 |

Introduction

The formation and evolution of the Milky Way galaxy is one of the greatest outstanding questions of astrophysics. According to the Λ CDM cosmological model (Mo et al. 1998; Silk & Bouwens 2001), large galaxies like our Galaxy emerge as an end-point of hierarchical clustering, merging and accretion. But we still lack of the detailed physical picture of how individual stellar populations can be associated with elements of the proto-cloud, and how different Galactic components formed and evolved. Even the thick disc, as a unique Galactic component discovered more than 30 years ago (Gilmore & Reid 1983), still has no approved formation scenario. Separation of the Galactic disc into "thick" and "thin" disc populations refers to different types of stars. Thick-disc stars are essentially older and more highly enriched in α -elements than thin-disc stars (Soubiran & Girard 2005). The enhancement in α -elements suggests that the thick-disc stars were formed on relatively short timescales (~ 1 Gyr), thus offering us a hint to the formation history of our Galaxy (Kordopatis et al. 2013a). Ancient minor mergers of satellite galaxies are considered as one possible scenario of the thick-disc formation.

Numerical simulations of merger events have shown that such debris streams survive as coherent structures over gigayears (Helmi 2004; Law et al. 2005; Peñarrubia et al. 2005). Stellar streams may be discovered as overdensities in the phase space distribution of stars in the solar vicinity. Examining the GCS catalogue, Helmi et al. (2006) looked for stellar streams in a space of orbital apocentre, pericentre and z -angular momentum (L_z), the so-called APL-space. In this kind of space stellar streams cluster around lines of constant eccentricity. They found three new coherent stellar groups (Group 1, 2, and 3) with distinctive ages, metallicities and kinematics, and suggested that those groups might correspond to remains of disrupted satellites.

A combined study of kinematics and chemical composition of stars is one of the most promising tools of research in galaxy formation. The main goal in this field of research is to reconstruct the formation history of our Galaxy, to reveal the origin of the thick disc, and to find remnants of ancient mergers. Large surveys, such as the Geneva Copenhagen Survey (GCS, Nordström et al. 2004), the RAdial Ve-

locity Experiment (RAVE, Steinmetz et al. 2006; Zwitter et al. 2008; Siebert et al. 2011), and the Sloan Extension for Galactic Understanding and Exploration (SEGUE, Yanny et al. 2009), are very useful databases for such studies. Large and deep chemodynamical surveys such as *Gaia* (Perryman et al. 2001) will enable us to characterise the Galaxy more precisely and to examine its formation scenarios as well as kinematic stellar group identification methods.

An indispensable method to check the origin of various kinematic streams is the investigation of their chemical composition. In this work we present the detailed chemical composition of stars belonging to Group 1 and Group 2 of the Geneva-Copenhagen survey, which were identified by Helmi et al. (2006). Despite the fact that the kinematic group members, over time, were dispersed through the Galactic disc, the chemical composition should remain unchanged. The high-resolution spectroscopic analysis is an important supplemental method in revealing and confirming the origin and history of GCS stellar groups.

Aims of the study

The main aim of the study is to perform a high-resolution spectroscopic analysis of the kinematic Group 1 and Group 2 of the Geneva-Copenhagen survey and to compare the results with Galactic thin-disc and thick-disc dwarfs, and thin-disc chemical evolution models.

The secondary goal is to investigate the homogeneity of the chemical composition of stars within each group and to look for possible chemical signatures that might give information about the formation history of those kinematic groups of stars.

Tasks of the study

- Determination of the main atmospheric parameters (effective temperature, surface gravity, metallicity and microturbulence) in the kinematically identified groups of stars and Galactic thin- and thick-disc comparison stars.
- Detailed chemical abundance determination of oxygen, α -elements, iron group and neutron capture chemical elements in Group 1 and Group 2 stars and comparison Galactic thin- and thick-disc stars.

- Interpretation of the results by comparing them with the Galactic disc dwarfs and chemical evolution models.
- Comparison of the chemical composition with other kinematic substructures.

Scientific novelty

- For the first time, the detailed high-resolution spectroscopic analysis is performed for the kinematic Group 1 and Group 2 northern hemisphere stars of the Geneva-Copenhagen Survey identified in the Galactic disc and suspected to be remnants of disrupted satellite galaxies.
- It is shown that the detailed chemical composition of the kinematic Group 1 and Group 2 stars of the Geneva-Copenhagen Survey is similar to the thick-disc stars, which might suggest that their formation histories are linked.
- The comparison of the chemical composition and kinematic properties showed, that the GCS kinematic stellar groups are different from Galactic streams which origin is associated with dynamical interactions between stars in the outer disc and the Galactic bar.
- We redetermined ages for one of the investigated GCS kinematic group.

Results and statements presented for defense

- The atmospheric parameters (effective temperature, surface gravity, and microturbulence) and abundances of 22 chemical elements determined from high-resolution spectra in 37 Group 1 stars, 32 Group 2 stars, 15 comparison Galactic thin-disc stars, and in five comparison Galactic thick-disc stars .
- The average $[\text{Fe}/\text{H}]$ value of the 37 Group 1 stars is -0.20 ± 0.14 and the average $[\text{Fe}/\text{H}]$ value of the 32 Group 2 stars is -0.42 ± 0.10 . The stars in the kinematically identified groups are chemically homogeneous.
- All programme stars are overabundant in oxygen, α -elements, and elements produced predominantly by the r-process compared with Galactic thin-disc dwarfs, and this abundance pattern has similar characteristics as the Galactic thick disc.

- The abundances of iron-group elements and chemical elements produced mainly by the s-process are similar to those in the Galactic thin-disc dwarfs of the same metallicity.
- The chemical composition patterns in GCS Groups 1, 2, and 3 are similar to each other and to the thick-disc stars, which might suggest that their formation histories are linked.
- Most of the Group 1 and Group 2 stars consist of two age 8- and 12-Gyr-old populations.
- The chemical composition and kinematic properties in the GCS Group 1, 2, and 3 stars are different from those in stars of the Hercules, Arcturus and AF06 streams.
- The chemical composition together with the kinematic properties and ages of stars in the investigated Groups 1, 2 and 3 of the Geneva-Copenhagen survey support a gas-rich satellite merger scenario a possible origin for these kinematic groups.

Personal contribution

The author, together with co-authors, prepared the observation programmes and observed some of the spectra with the Nordic Optical Telescope. The author made the reduction of spectra of observed stars, determined the main atmospheric parameters (effective temperature, surface gravity, metallicity and microturbulence) and chemical composition of the programme stars. The author interpreted the chemical composition results, drew conclusions and, together with co-authors, prepared scientific publications.

Publications on the subject of the dissertation

A list of publications contains 9 publications, 7 of them are included to the database of *Thomson Reuters Web of Science*.

1. Stonkutė, E., Tautvaišienė, G., Nordström, B. & **Ženovienė, R.**, 2012, *Chemical Composition of a Kinematically Identified Stellar Group in the Milky Way*, in *Star Clusters in the Era of Large Surveys* (eds. A. Moitinho, J. Alves), The Astrophysics and Space Science series, Proceedings of Symposium 5 of JENAM 2010, 223–224.
2. Stonkutė E., **Ženovienė R.**, Tautvaišienė G., Nordström B., 2012, *Chemical analysis of ancient relicts in the Milky Way disk*, in „Assembling the Puzzle of the Milky Way“ (eds. C. Reylé, A. Robin, M. Schultheis), European Physical Journal Web of Conferences, Vol. 19, 05007 1–2.
3. Stonkutė E., Tautvaišienė G., Nordström B., **Ženovienė R.**, 2012, *Stellar substructures in the solar neighbourhood. I. Kinematic group 3 in the Geneva-Copenhagen survey*, *Astronomy & Astrophysics*, Vol. 541, A157, 1–9.
4. Nordström B., Stonkutė E., Tautvaišienė G., **Ženovienė R.**, 2012, *Chemical tagging of kinematic stellar groups in the Milky Way Disk*, in 3rd Subaru International Conference „Galactic Archeology: Near-Field Cosmology and the Formation of the Milky Way“ (eds. W. Aoki, N. Arimoto, M. Ishigaki, T. Suda, T. Tsujimoto), *Astronomical Society of the Pacific Conference Series*, Vol. 458, 235.
5. Stonkutė E., Tautvaišienė G., Nordström B., **Ženovienė R.**, 2013, *Stellar substructures in the solar neighbourhood: II. Abundances of neutron-capture elements in the kinematic Group 3 of the Geneva-Copenhagen survey*, *Astronomy & Astrophysics*, Vol. 555, A6, 1–8.
6. Nordström B., Stonkutė E., **Ženovienė R.**, Tautvaišienė G., 2014, *Traces of the formation history of the Milky Way*, in *Setting the Scene for GAIA and LAMOST* (eds. S. Feltzing, G. Zhao, N. A. Walton, P. Whitelock), *Proceedings of the International Astronomical Union, IAU Symposium*, Vol. 298, 430.
7. **Ženovienė R.**, Tautvaišienė G., Nordström B., Stonkutė E., 2014, *Stellar substructures in the solar neighbourhood: III. Kinematic group 2 in the Geneva-Copenhagen survey*, *Astronomy & Astrophysics*, Vol. 563, A53, 1–14.

8. **Ženovienė R.**, Stonkutė E., Tautvaišienė G., Nordström B., 2014, *Abundances of heavy elements in the kinematic stellar substructures*, *Memorie della Società Astronomica Italiana*, Vol. 85, 608–611.
9. **Ženovienė R.**, Tautvaišienė G., Nordström B., Stonkutė E., and Barisevičius G., 2015, *Stellar substructures in the solar neighbourhood: IV. Kinematic group 1 in the Geneva-Copenhagen survey*, *Astronomy & Astrophysics*, (in press).

Presentations at the international conferences

1. Stonkutė E., Tautvaišienė G., Nordström B., **Ženovienė R.**, *Chemical composition of a kinematically identified stellar group in the Milky Way*, Symposium 5 „Star Clusters in the Era of Large Surveys” of European Week of Astronomy and Space Science, JENAM 2010, Lisbon (Portugal), 6–10 September, 2010 (poster presentation).
2. Stonkutė E., Tautvaišienė G., Nordström B., **Ženovienė R.**, *Chemical composition of kinematically identified Galactic stellar groups*, „Seventh International Conference on Atomic and Molecular Data and Their Applications”, Vilnius (Lithuania), 21–24 September, 2010 (poster presentation).
3. Stonkutė E., **Ženovienė R.**, Tautvaišienė G., Nordström B., *Chemical analysis of ancient relicts in the Milky Way disk*, International conference „Assembling the Puzzle of the Milky Way”, Le Grand Bornand (France), 17–22 April, 2011 (poster presentation).
4. Nordström B., Stonkutė E., Tautvaišienė G., **Ženovienė R.**, *Chemical tagging of kinematic stellar groups in the Milky Way Disk*, The 3rd Subaru International Conference „Galactic Archaeology: Near – Field Cosmology and the Formation of the Milky Way”, Shuzenji (Japan), 01–04 November, 2011 (poster presentation).
5. **Ženovienė R.**, Tautvaišienė G., Stonkutė E., Nordström B., *A new kinematically identified stellar group: chemical composition study*, International conference „Science Innovation and Gender 2011”, Vilnius (Lithuania), 24–25 November, 2011 (poster presentation).

6. **Ženovienė R.**, Tautvaišienė G., Nordström B., Stonkutė E., *Chemical analysis of a new kinematically identified stellar group*, Symposium 6 „Stellar Populations 55 years after the Vatican Conference” of European Week of Astronomy and Space Science Science, EWASS 2012, Rome (Italy), 01–06 July, 2012 (poster presentation).
7. Stonkutė E., Tautvaišienė G., **Ženovienė R.**, Nordström B., *Chemical imprints of past accretion events in the Galaxy*, Special Sesion 3 „Galaxy evolution through secular processes” of IAU XXVIII General Assembly 2012, Beijing (China), 20–31 August, 2012 (poster presentation).
8. Nordström B., Stonkutė E., **Ženovienė R.**, Tautvaišienė G., *Traces of the formation history of the Milky Way*, IAU Symposium No. 298: „Setting the scene for Gaia and LAMOST”, Lijiang (China), 20–24 May, 2013 (poster presentation).
9. Tautvaišienė G., Stonkutė E., **Ženovienė R.**, Nordström B., *Spectral investigations of kinematic Galactic substructures*, „40-oji Lietuvos nacionalinė fizikos konferencija”, Vilnius (Lithuania), 10–20 June, 2013 (oral presentation).
10. **Ženovienė R.**, Stonkutė E., Tautvaišienė G., Nordström B., *Abundances of heavy elements in the kinematic stellar substructures*, Symposium 5 „Local Group, Local Cosmology” of European Week of Astronomy and Space Science Science, EWASS 2013, Turku (Finland), 8–12 July, 2013 (poster presentation).
11. **Ženovienė R.**, Tautvaišienė G., Stonkutė E., Bertašius V., *Chemical composition of a kinematic stellar groups in the solar neighbourhood*, 58th Scientific Conference for Students of Physics and Natural Sciences „Open Readings 2014”, Vilnius (Lithuania), 19–21 March, 2014 (oral presentation).

Thesis outline

The thesis work consists of introduction, three chapters, main results and conclusions, references, and appendices. Kinematic groups of stars are presented in the first chapter, observations and methods of analysis are described in the second chapter. The main atmospheric parameters and chemical composition of the Groups 1 and 2

stars and comparison with the Galactic thin- and thick-disc stars as well as with the kinematic stellar streams stars are presented and discussed in the third chapter of this thesis. At the end of this dissertation work are presented the main results and conclusions, the list of references, and two appendices.

Kinematic groups of stars

1.1 Kinematic stellar groups in the solar neighbourhood

Fine structures in the phase space distribution of nearby stars were first described by Eggen (1970). These appeared as overdensities in the distributions of the three space velocity components (U , V , W) and were called moving groups. Helmi and collaborators (Helmi et al. 1999; Helmi & de Zeeuw 2000, and references therein) have pointed out that kinematic groups can be detected equally well in orbital parameter spaces. Such groups represent ensembles of stars on similar orbits and are called by star streams.

In Helmi et al. (2006), streams among stars in the solar vicinity were specifically located in the space of perpendicular angular momentum L_z and pericenter and apocenter radii R_{peri} , R_{apo} of the stellar orbits, with $(R_{\text{apo}} - R_{\text{peri}})/(R_{\text{apo}} + R_{\text{peri}})$ being the eccentricity e of an orbit. Arifyanto & Fuchs (2006), Dettbarn et al. (2007), and Klement et al. (2008) proposed a projection of the e and L_z space, which according Dekker's (1976) theory of Galactic orbits can be approximated by $(U^2 + 2V^2)^{1/2}$ and V , respectively. The assumption is that stars in the same stellar stream move on orbits that stay close together, which is justified by numerical simulations of satellite disruptions (Helmi et al. 2006). With this method, Arifyanto & Fuchs (2006) identified several known streams (Hyades-Pleiades, Hercules, and Arcturus) and one new, the so-called AF06 stream (later confirmed by Klement et al. 2009 and by Klement et al. 2011).

Dettbarn et al. (2007) analysed the phase space distribution in a sample of non-kinematically selected low metallicity stars in the solar vicinity and determined the orbital parameters of several halo streams. One of those streams seemed to have precisely the same kinematics as the Sagittarius stream.

Klement et al. (2008) have searched for stellar streams or moving groups in

the solar neighbourhood, using the data provided by the first RAVE public data release. They estimated overdensities related to the Sirius, Hercules, Arcturus, and Hyades-Pleiades moving groups. Besides, they found a new stream candidate (KFR08), suggesting that its origin is external to the Milky Way’s disc. The KFR08 stream later was confirmed by Klement et al. (2009) and Bobylev et al. (2010). Antoja et al. (2012) also used the RAVE data and discovered a new group at $(U, V) = (92, -22) \text{ km s}^{-1}$ in the Solar neighbourhood. The new group was detected as a significant overdensity in the velocity distributions using a technique based on the wavelet transform.

A mechanism, known as ‘ringing’ was introduced by Minchev et al. (2009), it explains the presence of the moving groups detected by Arifyanto & Fuchs (2006) and Klement et al. (2008). Minchev et al. (2009) showed that the sudden energy kick imparted by the gravitational potential of the satellite as it crosses the plane of the disc can strongly perturb the velocity field of disc stars located in local volumes such as the solar neighbourhood. These perturbations can be observed in the (U, V) plane as arc-like features (see Gómez et al. 2012). Their simulations predicted the presence of four new streams with the predicted time of an impact of about 1.9 Gyr ago.

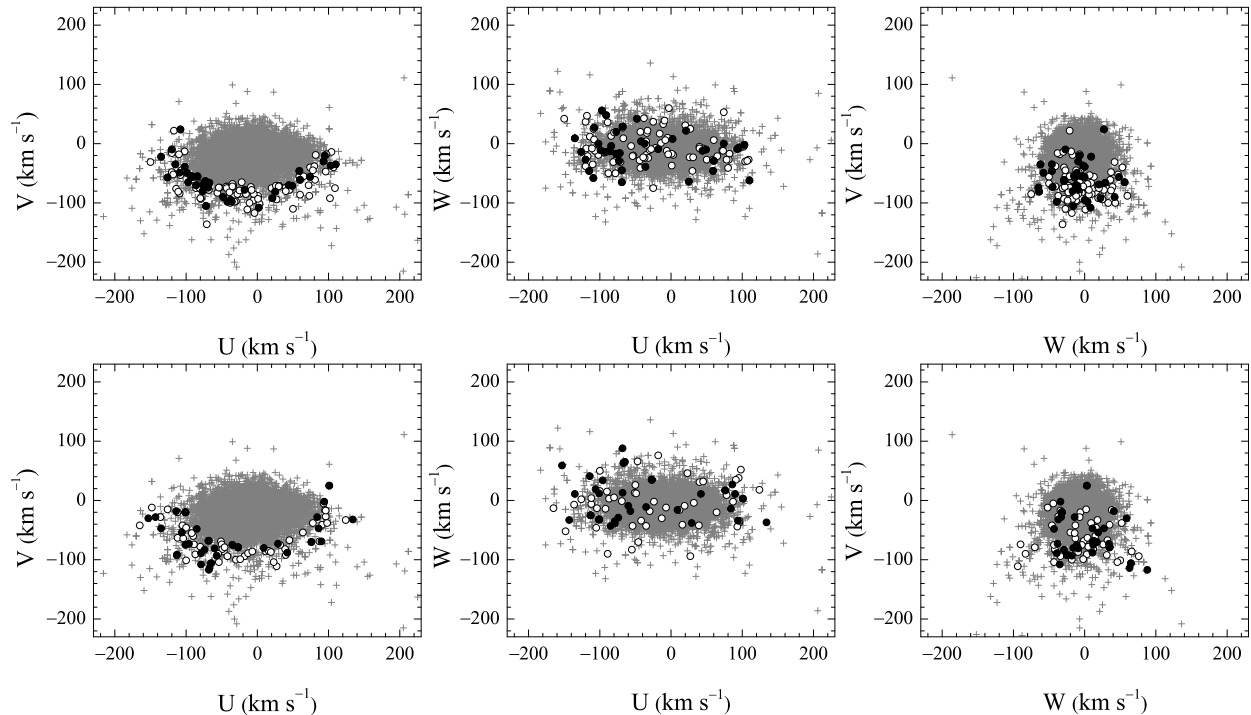
1.2 Kinematic Group 1 and Group 2 of the Geneva-Copenhagen Survey

Three investigated kinematic stellar groups were identified in the GCS catalogue by Helmi et al. (2006). The GCS provides metallicities, ages, kinematics, and Galactic orbits for a complete, magnitude-limited, all-sky sample of $\sim 14\,000$ F- and G-dwarfs brighter than $V \sim 8.3$. The basic observational data are Strömgren $uvby\beta$ photometry, Hipparcos/Tycho-2 parallaxes and proper motions, and some 63 000 new, accurate radial velocity observations, supplemented by earlier data. The best available calibrations were used to derive effective temperatures, metallicities, and distances. The astrometry and radial velocities were used to compute space motions and identify binaries in the sample. Finally, unbiased ages and error estimates were computed from a set of theoretical isochrones by a sophisticated Bayesian technique (Jørgensen & Lindegren 2005), and Galactic orbits were computed from the present

positions and velocity vectors of the stars and a Galactic potential model.

Helmi et al. (2006) analysed numerical simulations of the disruption of satellite galaxies and found substructures in the space defined by apocentre, pericentre, and z -angular momentum (the so called APL-space). Stars released in different perigalactic passages of the merging galaxy have slightly different orbital properties, and hence are located in several smaller lumps in the APL-space. However, these lumps are located along a segment of constant eccentricity, thereby permitting the assessment of a common origin. Such substructures in the APL-space remain coherent for many Gyr, well after the mergers have fully mixed. The APL-space for the GCS catalogue shows large amounts of substructures. The most prominent structures are related to the superclusters Hyades-Pleiades, Sirius and Hercules, and are most likely generated by dynamical perturbations induced by the spiral arms and the Galactic bar. These structures are composed of stars on disc-like orbits with relatively low eccentricity. However, the detailed statistical analysis of the APL-space revealed about ten other overdensities at significance levels higher than 99%. These overdensities were located along two to three segments of constant eccentricity, as predicted for substructures that are the result of minor mergers. There were 274 stars in this region of the APL-space, which is delimited by eccentricity $0.3 \leq e < 0.5$. The authors provide statistical evidence that these overdensities are real, they are not resulted by a poor choice of the comparison model of the Galaxy or uncertainties of eccentricity determinations. The metallicity distribution of the stars in this overdense region of the APL-space varied with eccentricity in a discontinuous fashion. This allowed the separation of these stars into three groups. These three groups of stars are dissimilar not only in their metallicity distribution, but also have different kinematics in the vertical (z) direction. The Group 1 has velocity dispersion σ_z about 28kms^{-1} , that of Group 2 about 39kms^{-1} , and that of Group 3 about 52kms^{-1} . The groups also have distinct age distributions.

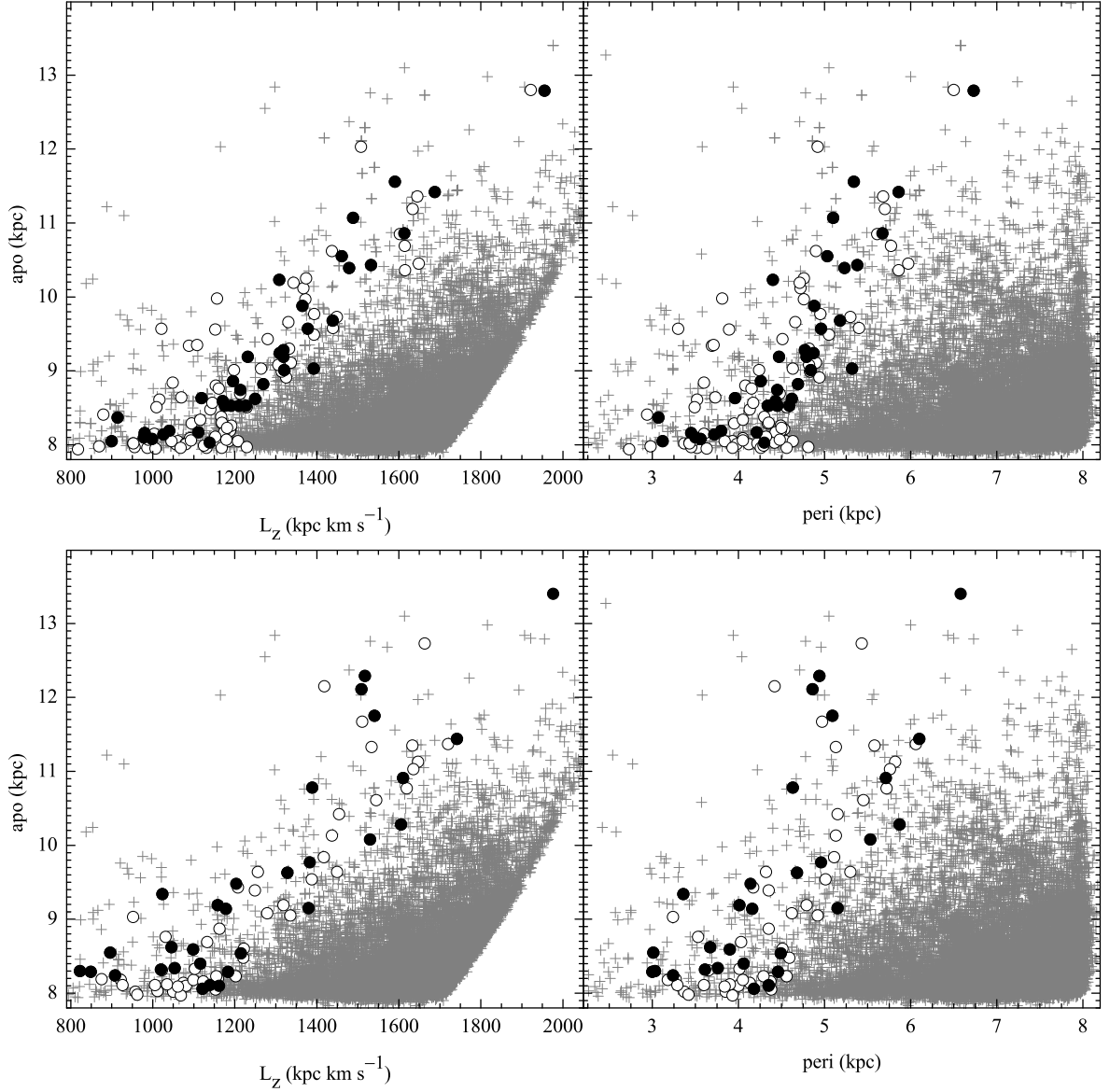
In the (U , V) plane (see Fig. 1.1), the investigated stars are distributed in a banana-shape, whereas the disc stars define a centrally concentrated clump. At the same time, in the (U , W) plane the investigated stars populate mostly the outskirts of the distributions. Both the U and W distributions are very symmetric. The investigated stars have a lower mean rotational velocity than the Milky Way disc stars, as we can see in the (W , V) plane. These characteristics are typical for stars associated with accreted satellite galaxies (Helmi 2008; Villalobos & Helmi 2009). An



1.1 Figure: Velocity distribution for all stars in the sample of Holmberg et al. (2009) (plus signs), stars in the kinematic group (circles), and the investigated stars (filled circles). Upper panel corresponds to Group 1, lower – to Group 2.

average error of stellar space motions in each component (U , V , and W) is 1.5 km s^{-1} (Nordström et al. 2004). In Fig. 1.2, the stars are shown in the APL space. The location of a star in the APL space is very accurate. A limited knowledge of the form of the Galactic potential, used to determine values of apocentre and pericentre, does not affect the distribution of points in the APL space much because the volume probed by the GCS sample is so small that the Galactic potential is close to a constant inside this region (c.f. Helmi et al. 2006). This implies that the energy, and hence the orbital parameters or the location of a star in the APL space, are determined mostly by its kinematics rather than by its spatial location (or the Galactic potential). Changes in the Galactic potential produce only small variations in the orbital parameters. According to Helmi et al. (2006), in the case of the potential proposed by Flynn et al. (1996), which was used for the orbit integrations in Nordström et al. (2004) and the following papers, a typical change in the apocentre and pericentre is of about 1–2%.

Stars in the identified groups cluster not only around regions of roughly constant eccentricity ($0.3 \leq e < 0.5$) and have distinct kinematics, but have also distinct me-



1.2 Figure: Distribution for the stars in the APL space. Plus signs denote the GCS sample (Holmberg et al. 2009), circles denote stars in the kinematic group, the filled circles are the investigated stars. Upper panel corresponds to Group 1, lower – to Group 2. Note that the investigated stars as well as all stars in the kinematic group are distributed in APL space with constant eccentricity.

tallicities $[\text{Fe}/\text{H}]$ and age distributions. One of the parameters according to which the stars were divided into three groups was metallicity. Group 3, the most metal-deficient, were investigated by Stonkutė et al. (2012, 2013). In this thesis work we investigated stars in Group 1 and Group 2. Group 1 is the most numerous and the most metal-rich of the GCS groups, it consist of 120 stars. According to the Holmberg et al. (2007) catalogue, its mean photometric metallicity, $[\text{Fe}/\text{H}]$, is about -0.45 dex. The Group 1 stars are distributed into two age populations of 8 Gyr and 12 Gyr. Group 2 contains 86 stars. Its mean photometric metallicity from the Holmberg et al. (2007) catalogue is about -0.6 dex. According to Helmi et al. (2006), the stars fall into three populations: 15% of the stars are 8 Gyr old, 36% are 12 Gyr old, and 49% are 16 Gyr old.

Observations and analysis

2.1 Observations

Spectra of high-resolving power ($R \approx 68000$) in the wavelength range of 3680–7270 Å were obtained at the Nordic Optical Telescope with the FIES spectrograph. All spectra were exposed to reach a signal-to-noise ratio higher than 100. Reductions of CCD images were made with the FIES pipeline FIEStool, which performs a complete reduction: calculation of reference frame, bias and scattering subtraction, flat-field division, wavelength calibration and other procedures¹.

Thirty-seven Group 1, thirty-two Group 2, fifteen comparison thin-disc, and five comparison thick-stars were observed.

2.2 Differential analysis

The spectra were analysed using a differential model atmosphere technique. This technique helps to eliminate systematic uncertainties. We performed the differential abundance analysis for all Group 1, Group 2 and comparison Galactic thin- and thick-disc stars relative to the Sun as a standard star.

Using solar equivalent widths of the same analysed lines from Gurtovenko & Kostyk (1989) we obtained the solar abundances, used later for the differential determination of abundances in the programme stars. We used the solar model atmosphere from the set calculated in Uppsala with a microturbulent velocity of 0.8 km s^{-1} , as derived from Fe I lines.

2.2.1 Software packages and model atmospheres

The EQWIDTH and BSYN program packages, developed at the Uppsala Astronomical Observatory, were used to carry out the calculation of abundances from measured

¹<http://www.not.iac.es/instruments/fies/fiestool>

equivalent widths and synthetic spectra, respectively.

EQWIDTH is a package for the calculation of elemental abundances from measured equivalent widths. Elemental abundances for Na, Al, α -elements and iron group chemical elements were determined by means of equivalent width measurements. The equivalent widths of the lines were measured by fitting of a Gaussian profile using the 4A (Ilyin 2000) or SPLAT² software packages.

Abundances of oxygen and neutron capture elements were determined using the spectrum synthesis BSYN package. BSYN calculates profiles of lines according to the input data and constructs a superposition of theoretical line profiles for all spectral lines presented in the wavelength range of the analysis.

A set of plane-parallel, line-blanketed, constant-flux local thermodynamical equilibrium (LTE) model atmospheres (Gustafsson et al. 2008) were taken from the MARCS stellar model atmosphere and flux library³.

2.2.2 Atomic data

The Vienna Atomic Line Data Base (VALD, Piskunov et al. 1995) was extensively used in preparing input data for the calculations. Atomic oscillator strengths for the main spectral lines analysed in this study were taken from an inverse solar spectrum analysis performed in Kiev (Gurtovenko & Kostyk 1989).

In addition to thermal and microturbulent Doppler broadening of lines, atomic line broadening by radiation damping and van der Waals damping were considered in calculating abundances. Radiation damping parameters of lines were taken from the VALD database. In most cases the hydrogen pressure damping of metal lines was treated using the modern quantum mechanical calculations by Anstee & O'Mara (1995), Barklem & O'Mara (1997), and Barklem et al. (1998). When using the Unsöld (1955) approximation, correction factors to the classical van der Waals damping approximation by widths (Γ_6) were taken from Simmons & Blackwell (1982). For all other species a correction factor of 2.5 was applied to the classical Γ_6 ($\Delta\log C_6 = +1.0$), following Mäckle et al. (1975). For the lines with equivalent widths stronger than 100 mÅ in the solar spectrum the correction factors were selected individually by inspecting the solar spectrum.

²<http://star-www.dur.ac.uk/~pdraper/splat/splat-vo.html>

³<http://marcs.astro.uu.se/>

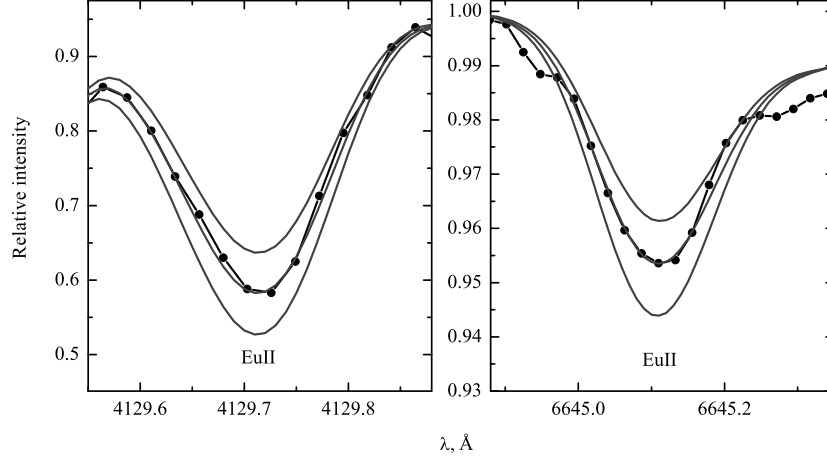
Non-local thermodynamical equilibrium. Abundances of Na and Mg were determined with non-local thermodynamical equilibrium (NLTE) taken into account, as described by Gratton et al. (1999). The calculated corrections did not exceed 0.04 dex for Na I and 0.06 dex for Mg I lines. Abundances of sodium were determined from equivalent widths of the Na I lines at 4751.8, 5148.8, 5682.6, 6154.2, and 6160.8 Å; magnesium from the Mg I lines at 4730.0, 5711.1, 6318.7, and 6319.2 Å.

2.2.3 Synthetic spectra

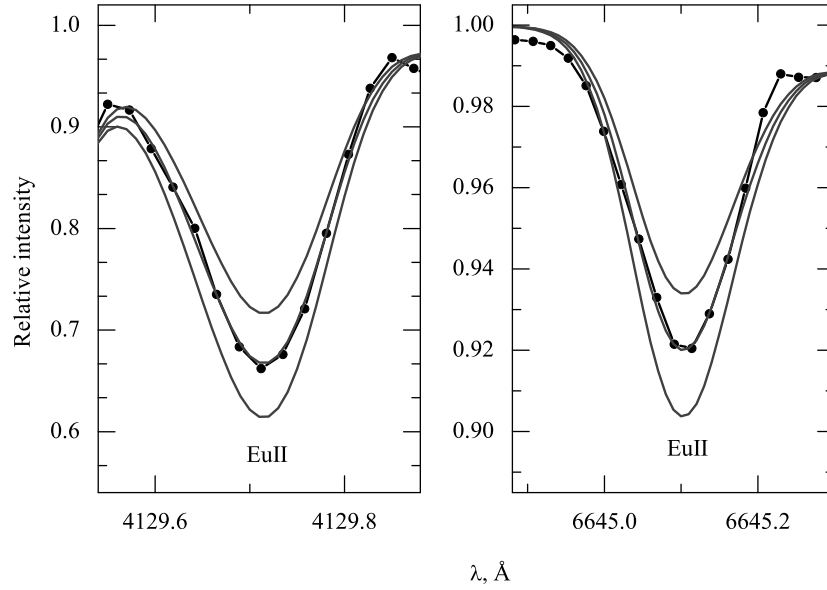
The oxygen abundance was determined from the forbidden [O I] line at 6300.31 Å. The oscillator strength values for ^{58}Ni and ^{60}Ni , which blend the oxygen line, were taken from Johansson et al. (2003). The [O I] $\log gf = -9.917$ value was calibrated by fitting to the solar spectrum (Kurucz 2005) with $\log A_{\odot} = 8.83$ taken from Grevesse & Sauval (2000).

Abundances of the investigated chemical elements were determined from up to seven Y II lines at 4883.7, 4982.1, 5087.4, 5200.4, 5289.8, 5402.8, and 5728.9 Å; from the Zr I lines at 4687.8, 4772.3, 4815.6, 5385.1, 6134.6, 6140.5, and 6143.2 Å and Zr II lines at 5112.3 and 5350.1 Å; from the Ba II line at 5853.7 Å with the hyperfine structure (HFS) and isotopic composition adopted from McWilliam (1998). The lanthanum abundance was determined from the La II lines at 4662.5, 4748.7, 5123.0, and 6390.5 Å. To analyse the 4662.5, 5123.0, and 6390.5 Å lines, we adopted the $\log gf$ from Lawler et al. (2001a) and HFS patterns from Ivans et al. (2006). The HFS patterns were not provided for the La II line at 4748.7 Å. This line is very weak, so the broadening by hyperfine splitting can be neglected. Up to five Ce II lines at 5274.2, 5330.5, 5512.0, 5610.3, and 6043.4 Å were used to determine the abundance of cerium. The praseodymium abundance was determined from the Pr II lines at 5259.7 and 5322.8 Å with the information on HFS taken from Sneden et al. (2009). We investigated Nd II lines at 4811.3, 5130.6, 5255.5, 5276.9, 5293.2, 5319.8, and 5385.9 ; Sm II lines at 4467.3, 4577.7, and 4791.6 Å. For the Sm II line at 4467.3 Å the $\log gf$ was taken from Lawler et al. (2006), and the HFS patterns from Roederer et al. (2008). For the remaining two lines a hyperfine structure was not taken into account since these lines are very weak and their hyperfine splitting can be neglected (cf. Mishenina et al. 2013).

The abundance of europium was determined from the Eu II lines at 4129.7 and



2.1 Figure: Synthetic spectrum fit to the europium lines at 4129 Å and 6645 Å. The observed spectrum for the programme star HD 149105 is shown as a solid line with dots. The dark grey solid lines are synthetic spectra with $[\text{Eu}/\text{Fe}] = 0.04 \pm 0.1$ and $[\text{Eu}/\text{Fe}] = 0.11 \pm 0.1$, for these two lines respectively.



2.2 Figure: Synthetic spectrum fit to the europium lines at 4129 Å and 6645 Å. The observed spectrum for the programme star HD 12782 is shown as a solid line with dots. The dark grey solid lines are synthetic spectra with $[\text{Eu}/\text{Fe}] = 0.40 \pm 0.1$ and $[\text{Eu}/\text{Fe}] = 0.45 \pm 0.1$, for these two lines respectively.

6645.1 Å. The $\log gf$ values for the Eu II lines and isotope fractions were adopted from Lawler et al. (2001b). An information on the HFS pattern for the Eu II line at 4129.7 Å was taken from Ivans et al. (2006), and for the line at 6645.1 Å from Biehl (1976). A partial blending of the Eu II line 6645.1 Å with weak Si I and Cr I lines at 6645.21 Å was taken into account.

Several fits of the synthetic Eu line profiles to the observed spectra are shown in Figs. 2.1 and 2.2.

2.2.4 Determination of main atmospheric parameters

Main atmospheric parameters (effective temperature T_{eff} , surface gravity $\log g$, metallicity $[\text{Fe}/\text{H}]$, and microturbulence velocity v_t) were determined using spectroscopic methods.

Effective temperature T_{eff} . Initial values of the effective temperatures for the programme stars were taken from Holmberg et al. (2009) and then carefully checked and corrected, if needed, by forcing Fe I lines to yield no dependency of iron abundance on excitation potential through changes to the model effective temperature.

Surface gravity $\log g$. We used the ionization equilibrium method to find surface gravities of the programme stars by forcing neutral and ionized iron lines to yield the same iron abundances.

Microturbulence velocity v_t . The derived abundance should be the same regardless of which line (strong or weak) was used for the analysis. Microturbulence velocity values corresponding to the minimal line-to-line Fe I abundance scattering were chosen as correct values.

2.2.5 Uncertainties

The uncertainties in abundances are due to several sources: uncertainties caused by analysis of individual lines, including random errors of atomic data and continuum placement and uncertainties in the stellar parameters. The sensitivity of the abundance estimates to changes in the atmospheric parameters by the assumed errors $\Delta[\text{El}/\text{H}]^4$ are illustrated in the dissertation for the Group 1 star HD 52711 and the Group 2 star HD 10519 (Tables 2.2 and 2.3). Clearly, possible parameter errors do

⁴We use the customary spectroscopic notation $[\text{X}/\text{Y}] \equiv \log_{10}(N_{\text{X}}/N_{\text{Y}})_{\text{star}} - \log_{10}(N_{\text{X}}/N_{\text{Y}})_{\odot}$.

not affect the abundances seriously; the element-to-iron ratios, which we use in our discussion, are even less sensitive.

The scatter of the deduced abundances from different spectral lines, σ , gives an estimate of the uncertainty due to the random errors. The mean value of σ is 0.05 dex, thus the uncertainties in the derived abundances that are the result of random errors amount to approximately this value.

Results and discussion

3.1 Main atmospheric parameters

The atmospheric parameters T_{eff} , $\log g$, v_t , $[\text{Fe}/\text{H}]$ and abundances of 21 chemical elements relative to iron, $[\text{El}/\text{Fe}]$, of the programme and comparison stars are presented in Tables 3.1, 3.2 and 3.3.

The element-to-iron abundance ratios were derived for Na I, Mg I, Al I, Si I, Ca I, Sc II, Ti I, Ti II, V I, Cr I, Fe I, Fe II, Co I, Ni I spectral lines using measured equivalent widths. For all other species investigated in this study ([O I], Y II, Zr I, Zr II, Ba II, La II, Ce II, Pr II, Nd II, Sm II, and Eu II) we used the spectral synthesis method.

The metallicities of Group 1 stars we investigated lie in an interval of $0.04 \geq [\text{Fe}/\text{H}] \geq -0.57$ with the average $[\text{Fe}/\text{H}]$ equal to -0.20 ± 0.14 (s.d.) dex. The metallicities of Group 2 stars lie in an interval of $-0.16 \geq [\text{Fe}/\text{H}] \geq -0.60$, with a mean of $[\text{Fe}/\text{H}] = -0.42 \pm 0.10$ (s.d.) dex.

The determined elemental abundance ratios of stars in the investigated stellar group and comparison thin disc stars are presented in the thesis appendix (Tables from B1 to B6).

3.2 Comparison with previous studies

Effective temperatures for all stars investigated here are also available in Holmberg et al. (2009) and Casagrande et al. (2011). Casagrande et al. (2011) provided astrophysical parameters for the Geneva-Copenhagen survey by applying the infrared flux method to determine the effective temperature. In comparison to Holmberg et al. (2009), stars in the catalogue of Casagrande et al. (2011) are on average 100 K hotter. For the Group 1 stars investigated here, our spectroscopic temperatures are on average 40 ± 70 K hotter than in Holmberg et al. (2009) and 40 ± 90 K cooler than in Casagrande et al. (2011). For the Group 2 stars our temperatures are on average

3.1 Table: Parameters of the Group 1 stars.

| Star | T_{eff} K | $\lg g$ | v_t km s ⁻¹ | [Fe/H] | σ_{FeI} | n_{FeI} | σ_{FeII} | n_{FeII} |
|-------------|-----------------------|---------|-----------------------------|--------|-----------------------|------------------|------------------------|-------------------|
| HD 3795 | 5360 | 3.7 | 1.0 | -0.57 | 0.05 | 31 | 0.04 | 6 |
| HD 4607 | 6200 | 3.8 | 1.2 | -0.08 | 0.05 | 25 | 0.03 | 6 |
| HD 15777 | 5800 | 4.2 | 1.0 | -0.33 | 0.04 | 28 | 0.04 | 6 |
| HD 22872 | 5980 | 4.0 | 1.1 | 0.04 | 0.05 | 34 | 0.02 | 8 |
| HD 25123 | 5880 | 3.9 | 1.1 | 0.02 | 0.04 | 37 | 0.06 | 8 |
| HD 40040 | 5740 | 4.0 | 1.1 | -0.24 | 0.05 | 37 | 0.05 | 7 |
| HD 49409 | 5770 | 4.1 | 0.9 | -0.23 | 0.05 | 32 | 0.04 | 6 |
| HD 52711 | 5870 | 4.1 | 1.0 | -0.08 | 0.05 | 38 | 0.03 | 7 |
| HD 60779 | 5990 | 4.1 | 0.9 | -0.10 | 0.05 | 36 | 0.04 | 8 |
| HD 67088 | 5610 | 4.0 | 0.8 | -0.04 | 0.04 | 37 | 0.03 | 7 |
| HD 67587 | 6030 | 3.8 | 1.1 | -0.25 | 0.05 | 34 | 0.05 | 8 |
| HD 76095 | 5720 | 4.1 | 1.0 | -0.19 | 0.04 | 35 | 0.05 | 8 |
| HD 77408 | 6340 | 4.2 | 1.1 | -0.11 | 0.04 | 25 | 0.04 | 7 |
| HD 78558 | 5640 | 4.0 | 0.9 | -0.41 | 0.05 | 36 | 0.04 | 7 |
| HD 88371 | 5630 | 4.2 | 0.8 | -0.23 | 0.04 | 38 | 0.06 | 8 |
| HD 88446 | 5990 | 3.9 | 1.2 | -0.39 | 0.05 | 34 | 0.03 | 8 |
| HD 90508 | 5760 | 4.1 | 1.0 | -0.26 | 0.04 | 37 | 0.05 | 8 |
| HD 109498 | 5810 | 4.2 | 1.0 | -0.11 | 0.06 | 30 | 0.06 | 6 |
| HD 111367 | 5830 | 4.0 | 1.0 | -0.06 | 0.05 | 34 | 0.05 | 8 |
| HD 135694 | 5520 | 3.9 | 0.9 | -0.23 | 0.06 | 24 | 0.06 | 5 |
| HD 138750 | 6130 | 3.8 | 1.1 | -0.18 | 0.05 | 33 | 0.04 | 8 |
| HD 140209 | 5710 | 4.0 | 1.1 | -0.14 | 0.05 | 28 | 0.03 | 5 |
| HD 149105 | 5930 | 3.8 | 1.0 | -0.05 | 0.04 | 30 | 0.02 | 7 |
| HD 149890 | 6030 | 4.0 | 1.1 | -0.20 | 0.05 | 33 | 0.03 | 6 |
| HD 156617 | 5780 | 3.9 | 1.0 | -0.03 | 0.04 | 33 | 0.03 | 7 |
| HD 156893 | 5300 | 3.8 | 0.9 | -0.21 | 0.04 | 36 | 0.03 | 8 |
| HD 157214 | 5640 | 4.0 | 0.8 | -0.36 | 0.04 | 33 | 0.02 | 6 |
| BD +40 3374 | 5050 | 4.6 | 0.8 | -0.43 | 0.05 | 31 | 0.06 | 4 |
| HD 171009 | 5840 | 4.0 | 1.0 | -0.35 | 0.04 | 32 | 0.04 | 6 |
| HD 171242 | 5920 | 3.8 | 0.9 | -0.22 | 0.06 | 22 | 0.05 | 6 |
| HD 178478 | 5550 | 3.6 | 1.0 | -0.50 | 0.03 | 24 | 0.04 | 5 |
| HD 188326 | 5310 | 3.8 | 0.9 | -0.18 | 0.05 | 35 | 0.04 | 6 |
| HD 206373 | 5900 | 3.8 | 1.1 | -0.16 | 0.04 | 26 | 0.02 | 5 |
| HD 210483 | 5850 | 4.0 | 0.9 | -0.04 | 0.04 | 29 | 0.06 | 4 |
| HD 211476 | 5840 | 4.2 | 0.9 | -0.10 | 0.05 | 32 | 0.03 | 7 |
| HD 217511 | 6460 | 3.7 | 1.4 | -0.12 | 0.03 | 20 | 0.05 | 6 |
| HD 219175 | 6050 | 4.2 | 0.9 | -0.24 | 0.05 | 30 | 0.03 | 5 |

3.2 Table: Parameters of the Group 2 stars.

| Star | T_{eff} K | $\lg g$ | v_t km s ⁻¹ | [Fe/H] | σ_{FeI} | n_{FeI} | σ_{FeII} | n_{FeII} |
|-------------|-----------------------|---------|-----------------------------|--------|-----------------------|------------------|------------------------|-------------------|
| BD +68 813 | 5820 | 4.4 | 1.2 | -0.48 | 0.05 | 29 | 0.05 | 6 |
| BD +31 3330 | 4830 | 4.4 | 0.8 | -0.32 | 0.03 | 31 | 0.04 | 5 |
| HD 10519 | 5680 | 3.8 | 0.9 | -0.52 | 0.04 | 33 | 0.05 | 7 |
| HD 12782 | 4980 | 3.4 | 1.1 | -0.48 | 0.04 | 35 | 0.03 | 7 |
| HD 16397 | 5750 | 4.1 | 1.1 | -0.47 | 0.04 | 35 | 0.05 | 7 |
| HD 18757 | 5600 | 4.1 | 0.8 | -0.25 | 0.04 | 34 | 0.01 | 7 |
| HD 21543 | 5640 | 4.1 | 1.0 | -0.53 | 0.04 | 34 | 0.05 | 7 |
| HD 24156 | 5470 | 3.9 | 0.9 | -0.43 | 0.05 | 38 | 0.02 | 7 |
| HD 29587 | 5660 | 4.2 | 0.9 | -0.51 | 0.04 | 34 | 0.06 | 7 |
| HD 30649 | 5770 | 4.1 | 0.9 | -0.45 | 0.04 | 36 | 0.02 | 7 |
| HD 37739 | 6280 | 3.8 | 1.0 | -0.41 | 0.05 | 24 | 0.05 | 5 |
| HD 38767 | 6170 | 3.6 | 1.0 | -0.55 | 0.05 | 26 | 0.06 | 5 |
| HD 96094 | 5970 | 4.1 | 1.1 | -0.31 | 0.05 | 26 | 0.04 | 6 |
| HD 114606 | 5600 | 4.2 | 0.9 | -0.50 | 0.05 | 31 | 0.05 | 7 |
| HD 121533 | 5600 | 4.0 | 1.0 | -0.37 | 0.05 | 28 | 0.04 | 6 |
| HD 131582 | 4770 | 4.3 | 0.8 | -0.36 | 0.03 | 37 | 0.02 | 5 |
| HD 132142 | 5180 | 4.3 | 0.8 | -0.35 | 0.03 | 34 | 0.05 | 7 |
| HD 133621 | 5650 | 3.7 | 1.0 | -0.40 | 0.05 | 34 | 0.06 | 7 |
| HD 137687 | 5070 | 3.6 | 0.8 | -0.56 | 0.03 | 29 | 0.02 | 6 |
| HD 139457 | 6000 | 3.9 | 1.2 | -0.43 | 0.06 | 24 | 0.04 | 7 |
| HD 143291 | 5280 | 4.4 | 0.7 | -0.33 | 0.03 | 36 | 0.05 | 6 |
| HD 152123 | 6040 | 3.7 | 1.2 | -0.16 | 0.05 | 23 | 0.05 | 6 |
| HD 156802 | 5660 | 3.9 | 0.9 | -0.37 | 0.05 | 32 | 0.04 | 7 |
| HD 158226 | 5740 | 4.0 | 1.1 | -0.47 | 0.05 | 30 | 0.03 | 7 |
| HD 165401 | 5770 | 4.3 | 0.8 | -0.33 | 0.05 | 34 | 0.05 | 7 |
| HD 170357 | 5710 | 3.9 | 0.9 | -0.34 | 0.04 | 31 | 0.06 | 6 |
| HD 190404 | 5000 | 4.5 | 0.8 | -0.58 | 0.04 | 35 | 0.03 | 5 |
| HD 200580 | 5860 | 3.9 | 1.0 | -0.56 | 0.05 | 28 | 0.03 | 7 |
| HD 201099 | 5890 | 3.8 | 1.0 | -0.40 | 0.05 | 31 | 0.04 | 7 |
| HD 215594 | 5810 | 3.8 | 1.0 | -0.26 | 0.04 | 33 | 0.03 | 7 |
| HD 221830 | 5720 | 4.1 | 1.0 | -0.37 | 0.05 | 32 | 0.05 | 7 |
| HD 224817 | 5720 | 3.7 | 0.8 | -0.60 | 0.04 | 31 | 0.04 | 5 |

3.3 Table: Parameters of the comparison stars.

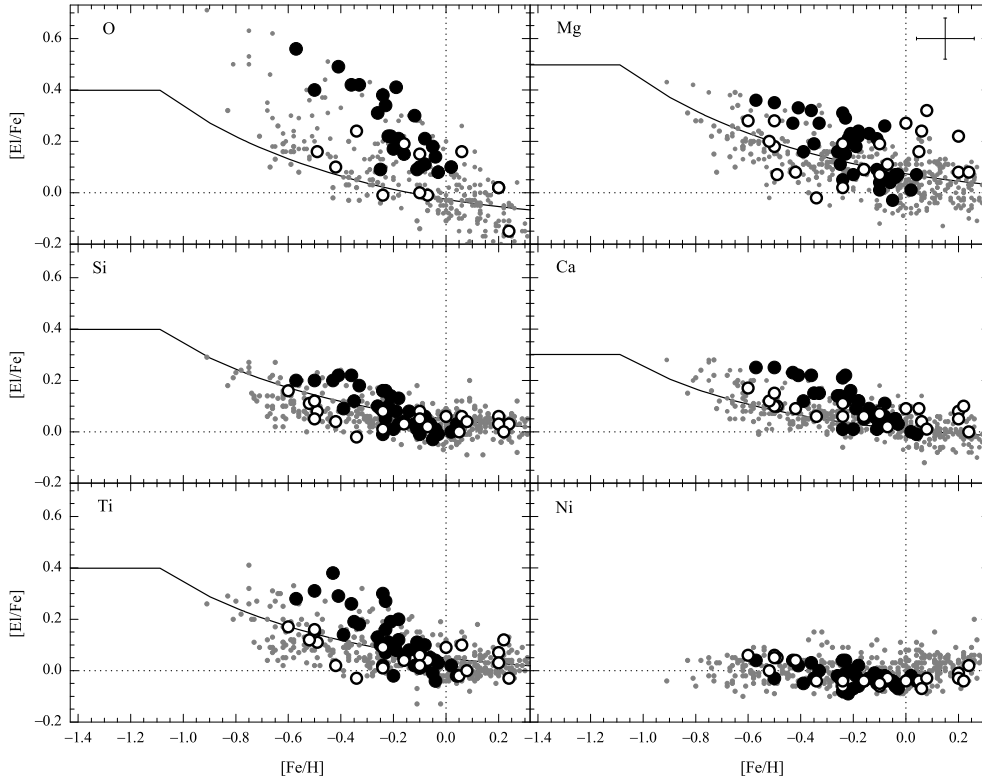
| Star | T_{eff} K | $\lg g$ | v_t km s ⁻¹ | [Fe/H] | σ_{FeI} | n_{FeI} | σ_{FeII} | n_{FeII} |
|------------------|-----------------------|---------|-----------------------------|--------|-----------------------|------------------|------------------------|-------------------|
| Thin disc stars | | | | | | | | |
| HD 41330 | 5820 | 4.0 | 1.0 | -0.16 | 0.04 | 35 | 0.03 | 7 |
| HD 43318 | 6230 | 3.6 | 1.1 | -0.10 | 0.05 | 29 | 0.05 | 6 |
| HD 69897 | 6330 | 4.0 | 1.3 | -0.24 | 0.05 | 38 | 0.02 | 7 |
| HD 108954 | 5960 | 3.9 | 1.1 | -0.07 | 0.05 | 29 | 0.03 | 6 |
| HD 115383 | 6090 | 4.0 | 1.2 | 0.20 | 0.05 | 29 | 0.05 | 8 |
| HD 127334 | 5610 | 4.0 | 0.8 | 0.24 | 0.05 | 33 | 0.07 | 7 |
| HD 136064 | 6090 | 3.9 | 1.1 | 0.05 | 0.06 | 30 | 0.04 | 7 |
| HD 153597 | 6380 | 4.0 | 1.3 | -0.10 | 0.05 | 20 | 0.05 | 5 |
| HD 157466 | 6130 | 4.2 | 1.2 | -0.34 | 0.05 | 30 | 0.05 | 7 |
| HD 163989 | 6240 | 3.7 | 1.3 | 0.06 | 0.04 | 30 | 0.03 | 8 |
| HD 176377 | 5770 | 4.1 | 0.8 | -0.24 | 0.05 | 37 | 0.05 | 7 |
| HD 187013 | 6290 | 3.6 | 1.3 | 0.00 | 0.05 | 22 | 0.04 | 7 |
| HD 187691 | 6140 | 3.9 | 1.2 | 0.20 | 0.05 | 35 | 0.05 | 8 |
| HD 200790 | 6190 | 3.9 | 1.3 | 0.08 | 0.04 | 32 | 0.02 | 8 |
| HD 220117 | 6480 | 3.4 | 1.2 | 0.22 | 0.04 | 23 | 0.04 | 6 |
| Thick disc stars | | | | | | | | |
| HD 150433 | 5650 | 4.2 | 0.9 | -0.34 | 0.05 | 37 | 0.05 | 7 |
| HD 181047 | 5550 | 4.2 | 0.8 | 0.01 | 0.05 | 35 | 0.04 | 6 |
| HD 186411 | 5860 | 3.7 | 1.2 | 0.11 | 0.05 | 34 | 0.03 | 8 |
| HD 195019 | 5750 | 4.0 | 0.9 | 0.11 | 0.03 | 37 | 0.04 | 8 |
| HD 198300 | 5830 | 4.1 | 0.9 | -0.44 | 0.04 | 38 | 0.04 | 8 |

only 10 ± 60 K hotter than in Holmberg et al. (2009) and 60 ± 80 K cooler than in Casagrande et al. (2011). The $[\text{Fe}/\text{H}]$ values for all of the stars we investigated are available in Holmberg et al. (2009) as well as in Casagrande et al. (2011). A comparison between Holmberg et al. (2009) and Casagrande et al. (2011) shows that the latter gives $[\text{Fe}/\text{H}]$ values that are more metal-rich on average by 0.1 dex. For our programme Group 1 and Group 2 stars we obtain a difference of 0.1 ± 0.1 dex in comparison with Holmberg et al. (2009) and we obtain no systematic difference, but a scatter of 0.1 dex, in comparison with Casagrande et al. (2011). The same result was found in comparing the atmospheric parameters determined for Group 3 stars in Stonkutė et al. (2012).

Some stars from our sample were previously investigated by other authors. We compare the results of Group 1 with Bensby et al. (2014) and Reddy et al. (2006), who investigated several stars in common with our work. The results of Group 2 compared with Reddy et al. (2006), Mashonkina et al. (2007), and Ramírez et al. (2007). Thirteen thin-disc stars that we investigated for a comparison have been analysed previously by Edvardsson et al. (1993), and two stars have been studied by Bensby et al. (2005). Slight differences in the $\log g$ values lie within the errors of uncertainties and are caused mainly by differences in the applied determination methods. We see that titanium and zirconium abundances determined using both neutral and ionised lines agree well and confirm the $\log g$ values determined using iron lines. Overall, our $[\text{El}/\text{Fe}]$ for the stars in common agree very well with those in other studies.

3.3 The detailed elemental abundances

The results are graphically displayed in Figs. 3.1, 3.2, 3.3, and 3.4. We display elemental abundance ratios of Group 1 and Group 2 stars together with data of thin-disc stars investigated here and in Stonkutė et al. (2012) and Stonkutė et al. (2013), as well as with results taken from thin-disc studies (Edvardsson et al. 1993; Gratton & Sneden 1994; Koch & Edvardsson 2002; Bensby et al. 2005; Zhang & Zhao 2006; Reddy et al. 2006; Brewer & Carney 2006; Mashonkina et al. 2007; Mishenina et al. 2013, and Bensby et al. 2014). The chemical evolution models of the thin-disc were taken from Pagel & Tautvaišienė (1995, 1997). The thin-disc stars from Edvardsson et al. (1993) and Zhang & Zhao (2006) were selected using the membership probability eva-

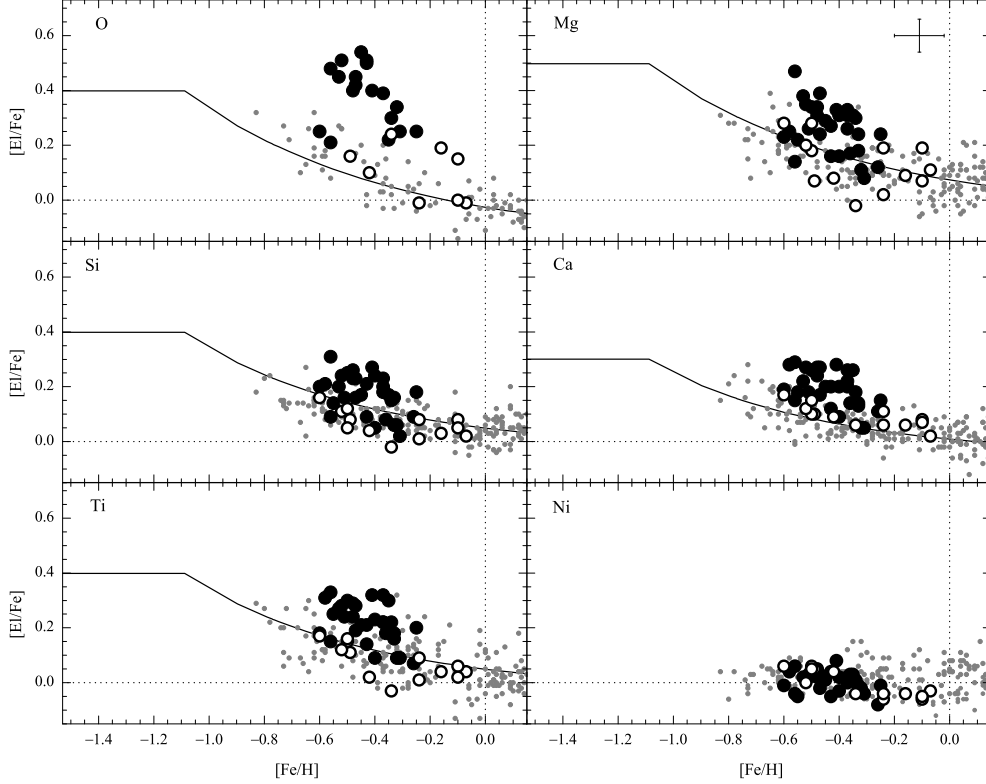


3.1 Figure: $[El/Fe]$ ratio as a function of $[Fe/H]$ for Group 1 stars (filled circles) investigated here and for comparison thin disc stars analysed in this work and Stonkutė et al. (2012) (open circles). The data for the Milky Way thin-disc dwarfs taken from other studies are shown as a grey dots. Solid lines are Galactic thin-disc chemical evolution models presented by Pagel & Tautvaišienė (1995). Average uncertainties are shown in the box for Mg.

luation method described by Trevisan et al. (2011), since their lists contained stars of other Galactic components as well. The same kinematic approach in assigning thin-disc membership was used in Bensby et al. (2005) and Reddy et al. (2006), which means that the thin-disc stars used for comparison are uniform in that respect.

One star in Group 1 is rich in elements produced in s-process. As shown in Fig. 3.3, star HD 88446 has much higher abundances of these elements. According to the definition of Beers et al. (2005), HD 88446, with its $[Ba/Fe] = 1.04$ and $[Ba/Eu] = 0.70$, falls in the category of the s-process-rich stars.

Two Group 2 stars (HD 200580 and HD 224817) have abundances of these elements similar to the thin-disc stars of the same metallicity. According to their element-to-iron ratios, these two stars might not belong to Group 2. However, their ages (~ 8 and 12 Gyr, respectively) as presented in 3.4 seem pretty old and similar to those of other member stars of Group 2. Their kinematic parameters are also similar to those of other stars in Group 2, therefore we have only one argument for

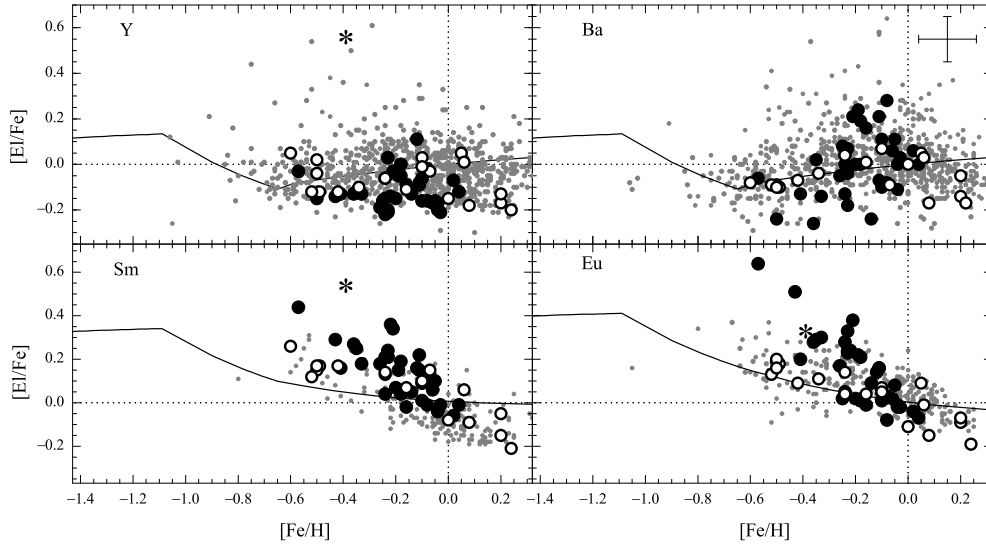


3.2 Figure: $[El/Fe]$ ratio as a function of $[Fe/H]$ for Group 2 stars (filled circles) investigated here and for comparison stars analysed in this work and Stonkutė et al. (2012) (open circles). The data for the Milky Way thin-disc dwarfs taken from other studies are shown as a grey dots. Solid lines are Galactic thin-disc chemical evolution models presented by Pagel & Tautvaišienė (1995). Average uncertainties are shown in the box for Mg.

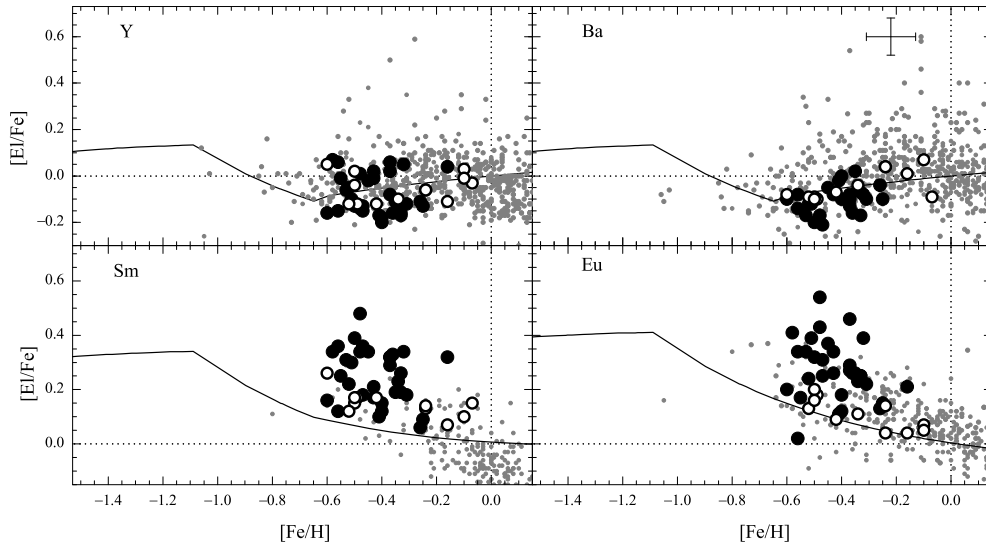
detracting a Group 2 membership from these two stars.

Abundances of chemical elements in the investigated Group 1 and Group 2 stars are rather homogeneous and show similar overabundances of α -elements and r-process-dominated chemical elements (particularly of Eu, Sm, and Pr) with respect to thin-disc stars, as we also found for the stars of GCS Group 3. This elemental abundance pattern has similar characteristics with that in the Galactic thick-disc.

In Table 3.4 we present a comparison of mean $[El/Fe]$ ratios calculated for stars of Group 1 and thick-disc stars at the same metallicity interval $-0.57 < [Fe/H] < 0.04$. Twenty-six thick-disc stars in this metallicity interval were investigated by Bensby et al. (2014), 37 stars by Reddy et al. (2006), 10 stars by Mashonkina et al. (2007), 51 stars by Stanford & Lambert (2012), and 7 stars by Mishenina et al. (2013). When comparing oxygen abundances, we did not use the results reported by Reddy et al. (2006) and Stanford & Lambert (2012) because they investigated the O I line, while



3.3 Figure: $[El/Fe]$ ratio as a function of $[Fe/H]$ for Group 1 stars (filled circles) investigated here and for comparison stars analysed in this work and Stonkutė et al. (2013) (open circles). The s-process enhanced star (HD 88446) is marked as an asterisk. Grey dots correspond to the data for the Milky Way thin-disc dwarfs taken from other studies. The Galactic thin-disc chemical evolution model is shown as a solid line (Pagel & Tautvaišienė, 1997). Average uncertainties are shown in the box for Ba.



3.4 Figure: $[El/Fe]$ ratio as a function of $[Fe/H]$ for Group 2 stars (filled circles) investigated here and for comparison stars analysed in this work and Stonkutė et al. (2013) (open circles). Grey dots correspond to the data for the Milky Way thin-disc dwarfs taken from other studies. The Galactic thin-disc chemical evolution model is shown as a solid line (Pagel & Tautvaišienė, 1997). Average uncertainties are shown in the box for Ba.

3.4 Table: Differences of mean [El/Fe] values for stars of Group 1 and thick-disc stars at the same metallicity interval $-0.57 < [\text{Fe}/\text{H}] < 0.04$.

| [El/Fe] | Ours-(a) B14 | Ours-(b) R06 | Ours-(c) Ma07 | Ours-(d) S12 | Ours-(e) Mi13 |
|---------|-----------------|-----------------|------------------|-----------------|------------------|
| [O/Fe] | -0.02 | ... | ... | ... | 0.08 |
| [Na/Fe] | -0.02 | -0.06 | ... | -0.02 | ... |
| [Mg/Fe] | -0.03 | -0.06 | ... | -0.01 | -0.03 |
| [Al/Fe] | -0.07 | -0.12 | ... | -0.07 | ... |
| [Si/Fe] | -0.04 | -0.10 | ... | -0.10 | -0.06 |
| [Ca/Fe] | 0.01 | -0.02 | ... | -0.02 | -0.04 |
| [Sc/Fe] | ... | -0.06 | ... | -0.11 | ... |
| [Ti/Fe] | -0.05 | -0.04 | ... | -0.01 | ... |
| [V/Fe] | ... | -0.06 | ... | -0.04 | ... |
| [Cr/Fe] | 0.01 | 0.03 | ... | -0.05 | ... |
| [Co/Fe] | ... | -0.06 | ... | -0.05 | ... |
| [Ni/Fe] | -0.03 | -0.05 | ... | -0.02 | -0.05 |
| [Y/Fe] | -0.09 | -0.08 | -0.13 | -0.11 | -0.11 |
| [Zr/Fe] | ... | ... | -0.07 | ... | 0.02 |
| [Ba/Fe] | 0.05 | 0.12 | 0.11 | 0.07 | 0.06 |
| [La/Fe] | ... | ... | ... | ... | 0.10 |
| [Ce/Fe] | ... | -0.07 | -0.06 | -0.08 | 0.02 |
| [Nd/Fe] | ... | -0.09 | ... | -0.06 | -0.05 |
| [Sm/Fe] | ... | ... | ... | ... | 0.02 |
| [Eu/Fe] | ... | -0.14 | ... | -0.17 | -0.06 |

(a) 63 stars from Bensby et al. (2014).

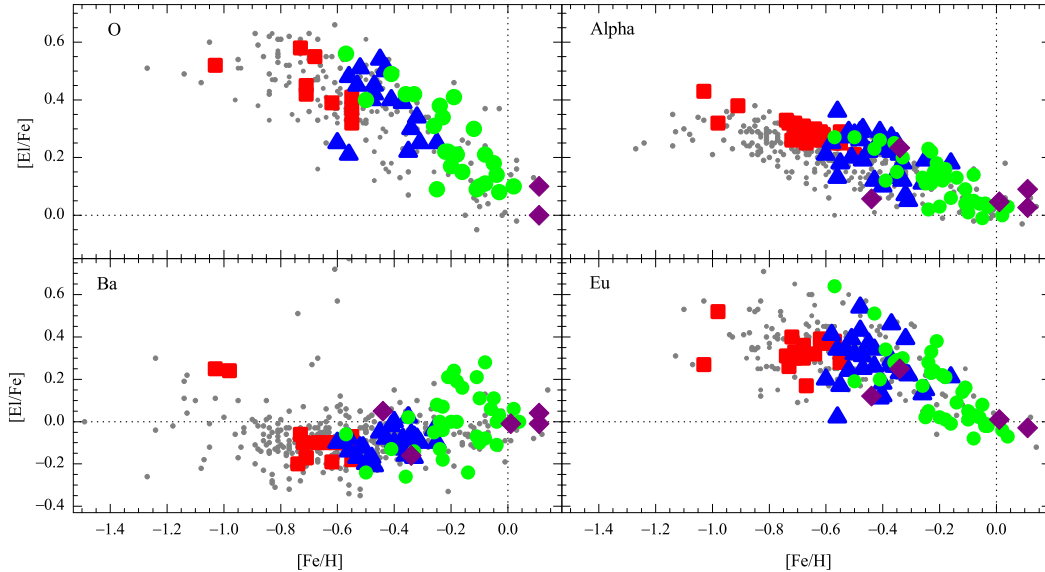
(b) 37 stars from Reddy et al. (2006).

(c) 10 stars from Mashonkina et al. (2007).

(d) 51 stars from Stanford & Lambert (2012).

(e) 10 stars from Mishenina et al. (2013).

we studied [O I]. We compare the mean [El/Fe] ratios calculated for stars of Group 2 and thick-disc stars at the same metallicity interval $-0.6 < [\text{Fe}/\text{H}] < -0.2$. Twenty-one stars in this metallicity interval were investigated by Bensby et al. (2005), 38 stars by Reddy et al. (2006), 11 stars by Mashonkina et al. (2007), and 7 stars by Mishenina et al. (2013). When comparing oxygen abundances, we did not use the results reported by Reddy et al. (2006) and neither did we use the results reported by Mishenina et al. (2013) because only three thick-disc stars fall in the corresponding metallicity interval. The comparison shows that the deviations do not exceed the uncertainties.

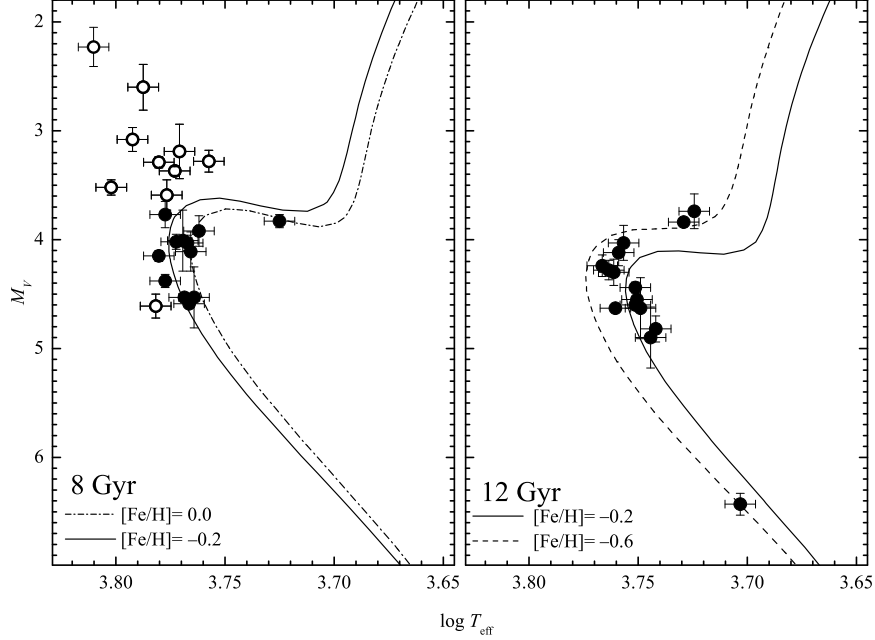


3.5 Figure: $[El/Fe]$ ratio as a function of $[Fe/H]$ in the Group 1 stars (green dots) investigated here, Group 2 (blue triangles), Group 3 (red squares, Stonkutė et al. (2012, 2013)), and comparison thick-disc stars (pink diamonds). The literature data for the Milky Way thick-disc stars are shown as a grey dots. The averaged values for α -elements consist of Mg, Si, and Ca abundances.

Fig. 3.5 displays the comparison of $[El/Fe]$ ratios for some chemical elements between individual stars in Groups 1, 2, and 3 and the thick-disc stars of the above-mentioned studies. For comparison we selected oxygen, the averaged values for the α -elements Mg, Si, and Ca, and the s- and r-process-dominated elements barium and europium. Stars of the kinematic groups and of the thick-disc have very similar chemical compositions. We have observed and analysed several thick-disc stars as well. Their elemental abundance ratios are also plotted in Fig. 3.5 and show a good agreement with the results of programme stars. Thus, the chemical composition of all three GCS kinematic groups is similar to the thick-disc stars, which might suggest that their formation histories are linked.

3.4 Age distribution

According to Helmi et al. (2006), the stars in Group 1 fall into two age populations: 33% of the stars are 8 Gyr old, and 67% are 12 Gyr old. The ages were later redetermined by Holmberg et al. (2009) and Casagrande et al. (2011) and agree with each other within uncertainties. Fig. 3.6 shows the Group 1 stars investigated here with

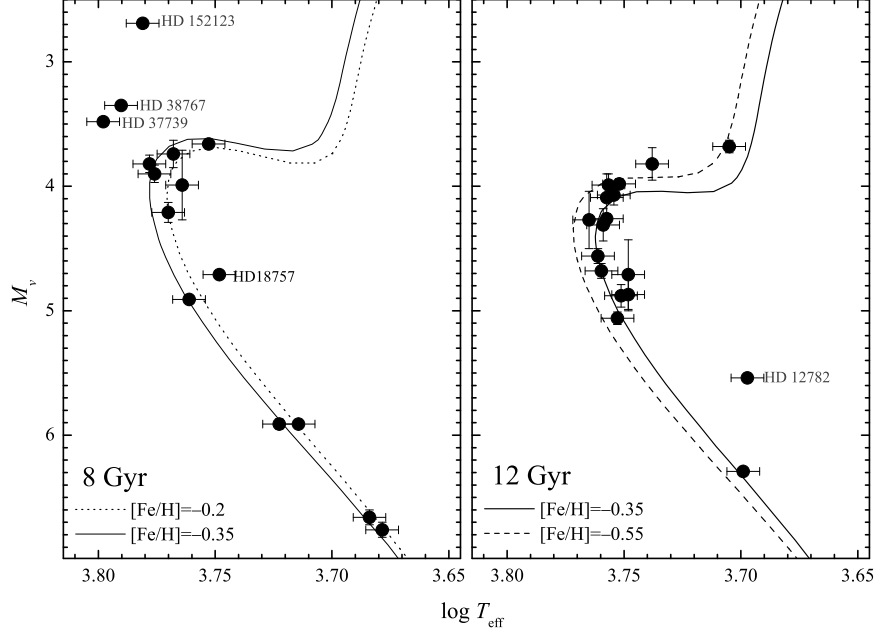


3.6 Figure: HR diagrams of the Group 1 stars. Isochrones are taken from Bressan et al. (2012). The isochrones for metal-deficient stars are with $[\alpha/\text{Fe}] = 0.2$. The open circles represent the younger stars with ages of 2–5 Gyr.

our spectroscopic effective temperatures and absolute magnitudes M_V , taken from Holmberg et al. (2009), in a Hertzsprung-Russell (HR) diagram. The isochrones were taken from Bressan et al. (2012). The overall features of stars in the diagrams are well reproduced by isochrones of the two indicated ages. The more metal-abundant stars fit the 8 Gyr isochrone quite well, while more metal-deficient stars fit the 12 Gyr isochrone (for metal-deficient stars, the isochrones are with $[\alpha/\text{Fe}] = 0.2$). A subgroup of ten stars in our sample are younger ($2 \text{ Gyr} \leq \text{age} \leq 5 \text{ Gyr}$) and in the HR diagram lie higher than the turnoff luminosity of the 8 Gyr isochrone.

Group 2 is characterised by an interesting feature related to the age distribution of its stars. According to Helmi et al. (2006), the stars fall into three populations: 15% of the stars are 8 Gyr old, 36% are 12 Gyr old, and 49% are 16 Gyr old. Because we redetermined the effective temperatures and metallicities using high-resolution spectra, we revisited the age determinations as well.

For the age determination we used the method by Jørgensen & Lindegren (2005) which was used previously in GCS studies (Helmi et al. 2006; Holmberg et al. 2009). This method and other similar Bayesian methods are currently the most common way to determine ages for larger stellar samples. This method with Bayesian probability functions gives a better understanding of how accurate the ages are. For the age



3.7 Figure: HR diagrams of the Group 2 stars. Isochrones are taken from Bressan et al. (2012). The filled circles correspond to the investigated stars with the spectroscopic effective temperatures. Isochrones are with $[\alpha/\text{Fe}] = 0.2$.

determination of Group 2 stars we took into account the $[\alpha/\text{Fe}]$ overabundance of 0.2 dex. The new age evaluations together with lower and upper age limits are presented in Table 3.5. Previously determined ages from Holmberg et al. (2009) and Casagrande et al. (2011) are presented as well.

Fig. 3.7 shows the Group 2 stars investigated here with our spectroscopic effective temperatures and absolute magnitudes M_v , taken from Holmberg et al. (2009), in a Hertzsprung-Russell (HR) diagram. The isochrones enhanced by $[\alpha/\text{Fe}] \sim 0.2$ were taken from Bressan et al. (2012). The overall features of stars in the diagram are well reproduced by isochrones of two ages. The more metal-abundant stars fit the 8 Gyr isochrone quite well, while more metal-deficient stars fit the 12 Gyr isochrone. Most of the stars for which older or younger ages were determined also fit these two age populations because these stars belong to the main sequence and determining their age accurately is problematic. As we can see from Fig. 3.7, the stars HD 37739, HD 38767, and HD 152123 are certainly younger ($2.5 \text{ Gyr} \leq \text{age} \leq 5 \text{ Gyr}$). In the HR diagram, they lie higher than the turnoff luminosity of the 8 Gyr isochrone. It seems that a subgroup of about 15 such young main sequence stars can be separated from 86 Group 2 stars. A chemical composition pattern of these young stars investigated in our work is similar to the rest of the Group 2 stars.

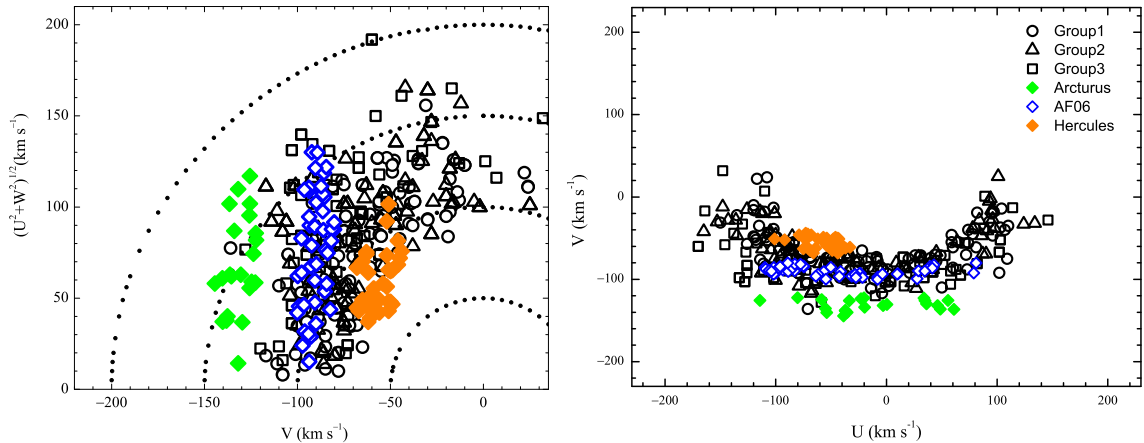
3.5 Table: Ages determined in this work and other studies. H09 – ages taken from Holmberg et al. (2009), C11 – from Casagrande et al. (2011), ages determined in this work together with lower and upper age limits are presented in the last three columns. All ages are in Gyr.

| Star | H09 | C11 | This work | -1σ | $+1\sigma$ |
|-------------|------|------|-----------|------------|------------|
| BD +68 813 | 13.3 | 9.2 | 9.8 | 7.5 | 11.8 |
| BD +31 3330 | ... | 7.1 | ... | ... | ... |
| HD 10519 | 12.4 | 11.8 | 12.0 | 10.9 | 13.1 |
| HD 12782 | ... | ... | ... | ... | ... |
| HD 16397 | 10.6 | ... | 10.4 | 7.9 | 12.4 |
| HD 18757 | 16.8 | ... | 11.0 | 8.9 | 16.2 |
| HD 21543 | 11.6 | 8.3 | 13.5 | 9.3 | 17.4 |
| HD 24156 | 11 | 10.2 | 10.4 | 8.9 | 11.8 |
| HD 29587 | 11.7 | 8.5 | 8.3 | 2.1 | 13.3 |
| HD 30649 | 10.1 | 7.8 | 9.8 | 8.1 | 12.5 |
| HD 37739 | 3.4 | 3.4 | 3.3 | 3.0 | 3.7 |
| HD 38767 | 4.9 | ... | 5.0 | 3.9 | 5.8 |
| HD 96094 | 8.6 | 8.7 | 6.3 | 4.9 | 7.9 |
| HD 114606 | 16.6 | 7.6 | 15.1 | 10.8 | 17.7 |
| HD 121533 | 12.6 | ... | 14 | 10.3 | 17.7 |
| HD 131582 | ... | ... | ... | ... | ... |
| HD 132142 | ... | 6.9 | 3.5 | 0.1 | 17.7 |
| HD 133621 | 11.8 | 10.5 | 10.9 | 10.0 | 11.7 |
| HD 137687 | ... | 7.1 | 8.7 | 7.9 | 9.9 |
| HD 139457 | 7.7 | 7.1 | 7.3 | 5.8 | 8.0 |
| HD 143291 | ... | 6.1 | ... | ... | ... |
| HD 152123 | 3.6 | 3.4 | 2.5 | 2.3 | 2.8 |
| HD 156802 | 9.7 | 7.9 | 9.1 | 7.3 | 11.3 |
| HD 158226 | 12.6 | 8.1 | 11.8 | 10.4 | 13.5 |
| HD 165401 | 8 | 5.1 | 2.5 | 0.1 | 7.5 |
| HD 170357 | 12.7 | 8.5 | 10.0 | 8.9 | 11.0 |
| HD 190404 | 0.2 | ... | 5 | 0.1 | 17.7 |
| HD 200580 | 8 | 8.4 | 8.4 | 7.6 | 9.4 |
| HD 201099 | 7.5 | 7.1 | 7.2 | 6.2 | 8.5 |
| HD 215594 | 10.2 | ... | 7.8 | 6.4 | 9.5 |
| HD 221830 | 12.4 | 9.3 | 11.5 | 10.2 | 12.9 |
| HD 224817 | 10.3 | 9.5 | 12.0 | 10.5 | 13.9 |

3.5 Comparison with kinematic streams

Our attention was attracted by the Hercules stream. Stars in this kinematic stream have a similar range of metallicities and ages to those in the GCS stellar groups (Bobylev & Bajkova 2007; Antoja et al. 2008; Bensby et al. 2007, 2014). The Hercules stream was first identified by Eggen (1958) as a group of 22 stars with velocities similar to the high velocity star ξ Herculis (HD 150680). It is believed that the Hercules stream is a result of resonant interactions between stars in the outer disc and the Galactic bar. This stellar stream is a heterogeneous group of objects from the thin and thick discs (Dehnen 2000; Fux 2001; Quillen 2003; Famaey et al. 2005; Soubiran & Girard 2005; Pakhomov et al. 2011; Antoja et al. 2014; Bensby et al. 2014).

The origin of the Arcturus stream has been debated for years (Eggen 1971, 1996, 1998; Arifyanto & Fuchs 2006; Gilmore et al. 2002; Wyse et al. 2006; Bensby et al. 2014, and references therein). Stars of the Arcturus stream were identified by Gilmore et al. (2002), and later Wyse et al. (2006), as a group of stars lagging behind the local standard of rest (LSR) by about 100 km s^{-1} . This stream was associated with a disrupted satellite that merged with the Milky Way 10–12 Gyr ago. Navarro et al. (2004) suggested that these stars are the same group of stars that Eggen (1971) associated with the bright star Arcturus, whose Galactic orbital velocity also lags at the same value. Navarro et al. (2004) analysed the group of stars associated kinematically with Arcturus and confirmed that they constitute a peculiar grouping of metal-poor stars with a similar apocentric radius, a common angular momentum, and distinct metal abundance patterns. These properties are consistent with those expected for a group of stars originating from the debris of a disrupted satellite. Navarro et al. (2004) also noticed that the angular momentum of such a group is too low to arise from dynamical perturbations induced by the Galactic bar. More recently, Gardner & Flynn (2010) and Monari et al. (2013) showed that the Galactic long bar may produce a kinematic feature in velocity space with the same parameters as occupied by the Arcturus moving group. Another so-called stellar stream AF06 was discovered by Arifyanto & Fuchs (2006) while analysing the fine structure of the phase space distribution function of nearby subdwarfs using data extracted from various catalogues. According to the discoverers, AF06 possibly resembles the Arcturus stream and probably has an extragalactic origin.

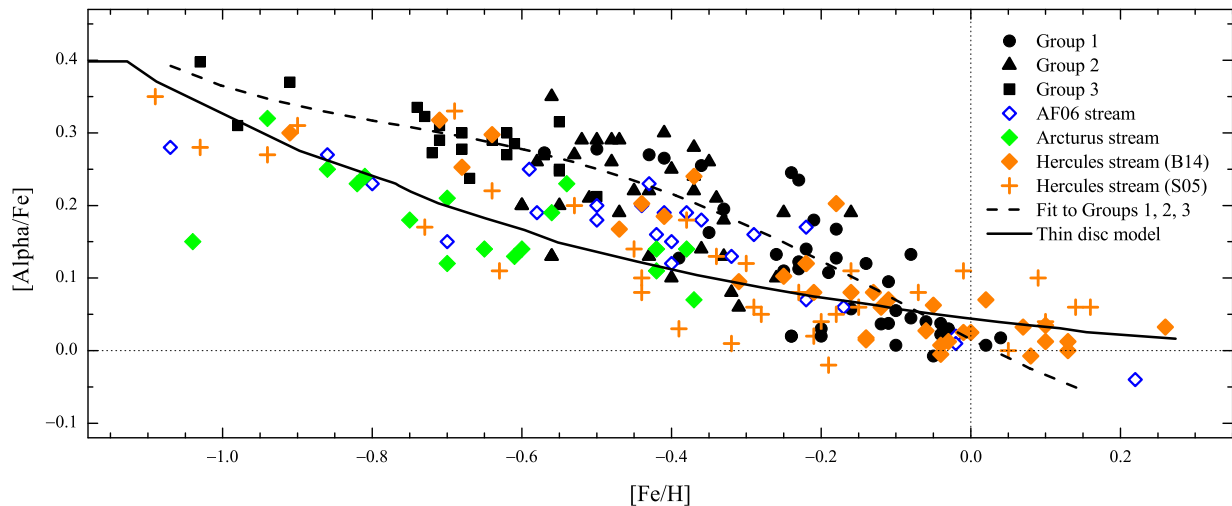


3.8 Figure: Left panel: Toomre diagram of stars in GCS kinematic groups and Arcturus, AF06, and Hercules streams. Dotted lines indicate constant values of space velocity V component in steps of 50 km s^{-1} . Right panel: Bottlinger diagram for stars in the same kinematic groups and streams.

Fig. 3.8 presents the Toomre diagram and the Bottlinger diagram of stars in the GCS kinematic groups and Hercules, Arcturus, and AF06 streams. These diagrams show that the kinematics of stars in the GCS groups is quite different from the displayed streams, and only AF06 partially overlaps the pattern.

A comparison of $[\text{El}/\text{Fe}]$ ratios for α -elements between individual stars in the GCS groups and stars of the Arcturus, AF06, and Hercules streams is presented in Fig. 3.9. The averaged values for α -elements consist of Mg, Si, Ca, and Ti abundances. The elemental abundances for 33 stars of the Hercules stream were taken from Soubiran & Girard (2005) and for 35 stars from Bensby et al. (2014). The elemental abundances for 18 stars of the Arcturus stream and for 26 stars of the AF06 stream were taken from Ramya et al. (2012). In Fig. 3.9 we also show the chemical evolution model of the Galactic thin-disc by Pagel & Tautvaišienė (1995) and a simple second-order polynomial fit to the GCS kinematic group stars.

The element-to-iron ratios in the GCS kinematic stellar groups lie higher than in the majority of stars belonging to Arcturus, AF06, and Hercules streams. The AF06 group has the chemical composition most similar to the GCS stars. The Arcturus group has thick-disc kinematics, however seemingly the thin-disc abundances. Finally, as noted previously, the stars associated with the Hercules stream do not have a distinct chemical signature, but show a mixture of abundances as seen in the thin and thick discs (e.g. Soubiran & Girard 2005; Bensby et al. 2007, 2014; Pakhomov et al. 2011).

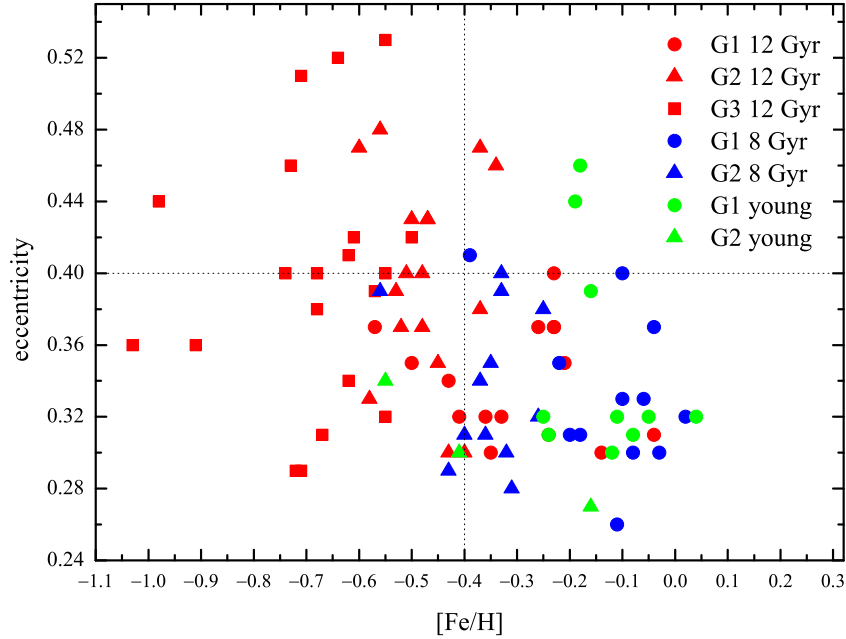


3.9 Figure: $[\alpha/\text{Fe}]$ ratio as a function of $[\text{Fe}/\text{H}]$ in the GCS kinematic group of stars, in the Arcturus stream (green diamonds), in the AF06 stream (blue empty diamonds), and in the Hercules stream (orange diamonds and crosses). The data for Arcturus and AF06 streams were taken from Ramya et al. (2012), for the Hercules stream from Soubiran & Girard (2005) and Bensby et al. (2014). The averaged values for α -elements consist of Mg, Si, Ca, and Ti abundances. A thin-disc model (continuous line) is taken from Pagel & Tautvaišienė (1995), the 2nd order polynomial fit to the GCS data is shown by the dashed line.

Thus, the presented comparison of kinematic and chemical composition patterns in the Galactic substructures, leads us to the conclusion that the origin of the GCS kinematic stellar groups was different from Galactic streams that originated in a course of the resonant interactions between stars in the outer disc and the Galactic bar.

3.6 Origin

Helmi et al. (2014) determined the detailed chemical composition for 36 stars of the GCS Group 1, for 22 stars of Group 2, and 14 stars of Group 3 located in the southern hemisphere. In this study, they noticed a relatively sharp transition in dynamical and chemical properties that occurs at a metallicity of $[\text{Fe}/\text{H}] \sim -0.4$. In their sample, stars with $[\text{Fe}/\text{H}] > -0.4$ have mostly lower eccentricities, smaller vertical velocity dispersions, are α -enhanced, and define a rather narrow sequence in $[\alpha/\text{Fe}]$ versus $[\text{Fe}/\text{H}]$, clearly distinct from that of the thin disc. Stars with $[\text{Fe}/\text{H}] < -0.4$ have a range of eccentricities, are hotter vertically, and depict a larger spread in $[\alpha/\text{Fe}]$. Looking at our slightly larger sample of GCS kinematic group stars (Fig. 3.10) inves-



3.10 Figure: Eccentricity and $[\text{Fe}/\text{H}]$ diagram of the GCS kinematic group stars. The red symbols correspond to stars investigated here with ages of about 12 Gyr, blue to about 8 Gyr, and green to the younger stars in Groups 1, 2, and 3.

investigated here, we agree with Helmi et al. (2014) that stars with lower metallicities have a wider range of eccentricities than those that are more metal-abundant. However, the spread of $[\alpha/\text{Fe}]$, seems about the same at all metallicities (see Fig. 3.5). In Fig. 3.10, we mark stars of different ages with different colours. Practically all stars with $[\text{Fe}/\text{H}] < -0.4$ have ages around 12 Gyr, while the youngest stars are predominantly metal-abundant.

Even though, according to the dynamical characteristics, the stars of the GCS kinematic groups do not constitute a homogeneous population, their similar chemical composition pattern indicates that these kinematic groups might share a similar origin. The similarity in chemical composition of stars in these kinematic groups and in the thick-disc of the Galaxy suggests that the formation histories of these groups and the thick-disc might be linked. This circumstance led us to look for the currently available thick-disc formation scenario, which allows for the presence of stars with GCS kinematic group characteristics. The kinematic properties of Groups 1, 2 and 3 fit a gas-rich satellite merger scenario well (Brook et al. 2004, 2005; Dierickx et al. 2010; Wilson et al. 2011; Di Matteo et al. 2011, and references therein). Within this specific scenario, the eccentricities of accreted stars peak at about $0.3 < e < 0.5$ (Sales et al. 2009), which are exactly the characteristics of the GCS groups that we

investigated. This scenario fits the thick-disc star eccentricity distribution better than the accretion, heating, or migration scenarios (Dierickx et al. 2010).

Dierickx et al. (2010) analysed the eccentricity distribution of thick-disc stars that has recently been proposed as a diagnostic to differentiate between these mechanisms (Sales et al. 2009). Using SDSS data release 7, they have assembled a sample of 31.535 G-dwarfs with six-dimensional phase-space information and metallicities and have derived their orbital eccentricities. They found that the observed eccentricity distribution is inconsistent with that predicted by orbital migration alone. Moreover, the thick-disc cannot be produced predominantly through heating of a pre-existing thin-disc, since this model predicts more high-eccentricity stars than observed. According to Dierickx et al. (2010), the observed eccentricity distribution fits a gas-rich merger scenario well, where most thick-disc stars were born *in situ*.

In the gas-rich satellite merger scenario, a distribution of stellar eccentricities peak around $e = 0.25$, with a tail towards higher values belonging mostly to stars originally formed in satellite galaxies. The groups of stars investigated in our work fit this model with a mean eccentricity value of 0.4. This scenario is also supported by the RAVE survey data analysis made by Wilson et al. (2011) and the numerical simulations by Di Matteo et al. (2011).

Finally, the numerical simulations of the disruption of a satellite galaxy that falls into its parent galaxy shows that the satellite debris can end up in several cold star streams with roughly the same characteristic eccentricities of their orbits (Helmi et al. 2006). The possibility of such a scheme and the similar properties of element-to-iron ratios found in the GCS kinematic groups lead to the assumption that the GCS kinematic star groups might belong to the same satellite galaxy and might have originated in our Galaxy during the same merging event.

Investigations of formation and evolution of the Milky Way discs are continuing both observationally (e.g. Haywood et al. 2013; Kordopatis et al. 2013b; Anders et al. 2014; Bensby et al. 2014; Bergemann et al. 2014; Mikolaitis et al. 2014) and theoretically (Micali et al. 2013; Snaith et al. 2014; Robin et al. 2014; Kubryk et al. 2014; Minchev et al. 2014, and references therein). A model that could reproduce well the present day values of all of the main global observables of the Milky Way disc has not been discovered yet. A number of formation scenarios for thick discs have been proposed. Although, it is likely that all of these processes to some extent act in the Milky Way, it is not clear which, if any, is the dominant mechanism.

Main results and conclusions

We measured abundances of 22 chemical elements from high-resolution spectra in 37 stars belonging to Group 1 and in 32 stars belonging to Group 2 of the Geneva-Copenhagen survey. These kinematically identified groups of stars as well as one other GCS kinematic group were suggested to be a remnant of a disrupted satellite galaxy. Our main goal was to investigate the chemical composition of stars within Group 1 and Group 2, to compare it with the relative abundance patterns in the Galactic thin- and thick-disc stars, in the GCS Group 3 stars, as well as in several kinematic streams of similar metallicities.

Our study shows the following:

1. The metallicities of the investigated stars in Group 1 are in the range $0.04 \geq [\text{Fe}/\text{H}] \geq -0.57$. The average $[\text{Fe}/\text{H}]$ value is -0.20 ± 0.14 dex. The metallicities of the investigated stars in Group 2 are in the range $-0.16 \geq [\text{Fe}/\text{H}] \geq -0.60$. The average $[\text{Fe}/\text{H}]$ value is -0.42 ± 0.10 dex.
2. All programme stars have higher abundances in oxygen, α -elements, and r-process-dominated chemical elements than Galactic thin-disc dwarfs and the Galactic evolution model, and this abundance pattern has similar characteristics as the Galactic thick disc.
3. The abundances of iron-group chemical elements and elements produced mainly by the s-process in accordance with the Galactic thick-disc are similar to those in the Galactic thin-disc dwarfs of the same metallicity.
4. The chemical composition patterns in GCS Groups 1, 2, and 3 are similar to each other and to the thick-disc stars, which might suggest that their formation histories are linked.
5. Most of the Group 1 and Group 2 stars consist of two age 8- and 12-Gyr-old populations.

6. The chemical composition and kinematic properties in GCS Groups 1, 2, and 3 stars are different from those in stars of the Hercules, Arcturus and AF06 streams.
7. The chemical composition together with the kinematic properties and ages of stars in the investigated GCS Groups 1, 2 and 3 support a gas-rich satellite merger scenario as a possible origin for these kinematic groups.

Bibliography

- Anders, F., Chiappini, C., Santiago, B. X., et al. 2014, *A&A*, 564, AA115
- Anstee S. D., O'Mara B. J., 1995, *MNRAS*, 276, 859
- Antoja, T., Figueras, F., Fernández, D., & Torra, J. 2008, *A&A*, 490, 135
- Antoja T., et al., 2012, *MNRAS*, 426, L1
- Antoja, T., Helmi, A., Dehnen, W., et al. 2014, *A&A*, 563, A60
- Arifyanto M. I., Fuchs B., 2006, *A&A*, 449, 533
- Barklem P. S., O'Mara B. J., 1997, *MNRAS*, 290, 102
- Barklem P. S., O'Mara B. J., Ross J. E., 1998, *MNRAS*, 296, 1057
- Beers T. C., Barklem P. S., Christlieb N., Hill V., 2005, *NuPhA*, 758, 595
- Bensby T., Feltzing S., Lundström I., Ilyin I., 2005, *A&A*, 433, 185
- Bensby, T., Oey, M. S., Feltzing, S., & Gustafsson, B. 2007, *ApJ*, 655, L89
- Bensby, T., Feltzing, S., & Oey, M. S. 2014, *A&A*, 562, A71
- Bensby T., Feltzing S., Lundström I., Ilyin I., 2005, *A&A*, 433, 185
- Bergemann, M., Ruchti, G. R., Serenelli, A., et al. 2014, *A&A*, 565, AA89
- Biehl D., 1976, PhD., Keele university
- Bobylev, V. V., & Bajkova, A. T. 2007, *Astronomy Reports*, 51, 372
- Bobylev, V. V., Bajkova, A. T., & Mylläri, A. A. 2010, *Astronomy Letters*, 36, 27
- Bressan A., Marigo P., Girardi L., Salasnich B., Dal Cero C., Rubele S., Nanni A., 2012, *MNRAS*, 427, 127
- Brewer M.-M., Carney B. W., 2006, *AJ*, 131, 431
- Brook C. B., Kawata D., Gibson B. K., Freeman K. C., 2004, *ApJ*, 612, 894
- Brook C. B., Gibson B. K., Martel H., Kawata D., 2005, *ApJ*, 630, 298

- Casagrande L., Schönrich R., Asplund M., Cassisi S., Ramírez I., Meléndez J., Bensby T., Feltzing S., 2011, *A&A*, 530, A138
- Dehnen, W. 2000, *AJ*, 119, 800
- Dekker, E. 1976, *Phys. Rep.*, 24, 315
- Dettbarn C., Fuchs B., Flynn C., Williams M., 2007, *A&A*, 474, 857
- Di Matteo P., Lehnert M. D., Qu Y., van Driel W., 2011, *A&A*, 525, L3
- Dierickx M., Klement R., Rix H.-W., Liu C., 2010, *ApJ*, 725, L186
- Edvardsson B., Andersen J., Gustafsson B., Lambert D. L., Nissen P. E., Tomkin J., 1993, *A&A*, 275, 101
- Eggen, O. J. 1958, *MNRAS*, 118, 154
- Eggen, O. J. 1970, *Vistas Astron.*, 12, 367
- Eggen, O. J. 1971, *PASP*, 83, 271
- Eggen, O. J. 1996, *AJ*, 112, 1595
- Eggen, O. J. 1998, *AJ*, 115, 2397
- Famaey, B., Jorissen, A., Luri, X., et al. 2005, *A&A*, 430, 165
- Flynn C., Sommer-Larsen J., Christensen P. R., 1996, *MNRAS*, 281, 1027
- Fux, R. 2001, *A&A*, 373, 511
- Gardner, E., & Flynn, C. 2010, *MNRAS*, 405, 545
- Gilmore, G., & Reid, N. 1983, *MNRAS*, 202, 1025
- Gilmore, G., Wyse, R. F. G., & Norris, J. E. 2002, *ApJ*, 574, L39
- Gómez, F. A., Minchev, I., Villalobos, Á., O'Shea, B. W., & Williams, M. E. K. 2012, *MNRAS*, 419, 2163
- Gratton R. G., Sneden C., 1994, *A&A*, 287, 927
- Gratton R. G., Carretta E., Eriksson K., Gustafsson B., 1999, *A&A*, 350, 955
- Grevesse N., Sauval A. J., 2000, *Origin of Elements in the Solar System, Implications of Post-1957 Observations, Proceedings of the International Symposium*. Edited by O. Manuel. Boston/Dordrecht: Kluwer Academic/Plenum Publishers, 261 p.

- Gurtovenko E. A., Kostyk R. I., 1989, Kiev, Izdatel'stvo Naukova Dumka, 200 p.
- Gustafsson B., Edvardsson B., Eriksson K., Jørgensen U. G., Nordlund Å., Plez B., 2008, *A&A*, 486, 951
- Haywood, M., Di Matteo, P., Lehnert, M. D., Katz, D., & Gómez, A. 2013, *A&A*, 560, AA109
- Helmi, A., Williams, M., Freeman, K. C., Bland-Hawthorn, J., & De Silva, G. 2014, *ApJ*, 791, 135
- Helmi A., 2008, *A&ARv*, 15, 145
- Helmi A., Navarro J. F., Nordström B., Holmberg J., Abadi M. G., Steinmetz M., 2006, *MNRAS*, 365, 1309
- Helmi, A. 2004, *ApJ*, 610, L97
- Helmi, A., & de Zeeuw, P. T. 2000, *MNRAS*, 319, 657
- Helmi, A., White, S. D. M., de Zeeuw, P. T., & Zhao, H. 1999, *Nature*, 402, 53
- Holmberg J., Nordström B., Andersen J., 2007, *A&A*, 475, 519
- Holmberg J., Nordström B., Andersen J., 2009, *A&A*, 501, 941
- Ilyin I. V., 2000, PhD, Oulu university
- Ivans I. I., Simmerer J., Sneden C., Lawler J. E., Cowan J. J., Gallino R., Bisterzo S., 2006, *ApJ*, 645, 613
- Jørgensen B. R., Lindegren L., 2005, *A&A*, 436, 127
- Johansson S., Litzén U., Lundberg H., Zhang Z., 2003, *ApJ*, 584, L107
- Klement, R., Fuchs, B., & Rix, H.-W. 2008, *ApJ*, 685, 261
- Klement R., et al., 2009, *ApJ*, 698, 865
- Klement, R. J., Bailer-Jones, C. A. L., Fuchs, B., Rix, H.-W., & Smith, K. W. 2011, *ApJ*, 726, 103
- Koch A., Edvardsson B., 2002, *A&A*, 381, 500
- Kordopatis, G., Hill, V., Irwin, M., et al. 2013a, *A&A*, 555, A12
- Kordopatis, G., Gilmore, G., Wyse, R. F. G., et al. 2013b, *MNRAS*, 436, 3231
- Kubryk, M., Prantzos, N., & Athanassoula, E. 2014, arXiv:1412.0585

Kurucz R. L., 2005, MSAIS, 8, 189

Law, D. R., Johnston, K. V., & Majewski, S. R. 2005, ApJ, 619, 807

Lawler J. E., Bonvallet G., Sneden C., 2001a, ApJ, 556, 452

Lawler J. E., Wickliffe M. E., den Hartog E. A., Sneden C., 2001b, ApJ, 563, 1075

Lawler J. E., Den Hartog E. A., Sneden C., Cowan J. J., 2006, ApJS, 162, 227

Mäckle R., Griffin R., Griffin R., Holweger H., 1975, A&AS, 19, 303

Mashonkina L. I., Vinogradova A. B., Ptitsyn D. A., Khokhlova V. S., Chernetsova T. A., 2007, ARep, 51, 903

Micali, A., Matteucci, F., & Romano, D. 2013, MNRAS, 436, 1648

Mikolaitis, Š., Hill, V., Recio-Blanco, A., et al. 2014, A&A, 572, AA33

Minchev I., Quillen A. C., Williams M., Freeman K. C., Nordhaus J., Siebert A., Bienaymé O., 2009, MNRAS, 396, L56

Minchev, I., Chiappini, C., & Martig, M. 2014, A&A, 572, AA92

Mishenina, T. V., Pignatari, M., Korotin, S. A., et al. 2013, A&A, 552, A128

McWilliam A., 1998, AJ, 115, 1640

Mo, H. J., Mao, S., & White, S. D. M. 1998, MNRAS, 295, 319

Monari, G., Antoja, T., & Helmi, A. 2013, arXiv:1306.2632

Navarro, J. F., Helmi, A., & Freeman, K. C. 2004, ApJ, 601, L43

Nordström B., et al., 2004, A&A, 418, 989

Pagal B. E. J., Tautvaisiene G., 1995, MNRAS, 276, 505

Pagal B. E. J., Tautvaisiene G., 1997, MNRAS, 288, 108

Pakhomov, Y. V., Antipova, L. I., & Boyarchuk, A. A. 2011, Astronomy Reports, 55, 256

Peñarrubia J., et al., 2005, ApJ, 626, 128

Perryman, M. A. C., de Boer, K. S., Gilmore, G., et al. 2001, A&A, 369, 339

Piskunov N. E., Kupka F., Ryabchikova T. A., Weiss W. W., Jeffery C. S., 1995, A&AS, 112, 525

Quillen A. C. 2003, *AJ*, 125, 785

Ramírez I., Allende Prieto C., Lambert D. L., 2007, *A&A*, 465, 271

Ramya, P., Reddy, B. E., Lambert, D. L. 2012, *MNRAS*, 425, 3188

Reddy B. E., Lambert D. L., Allende Prieto C., 2006, *MNRAS*, 367, 1329

Robin, A. C., Reylé, C., Fliri, J., et al. 2014, *A&A*, 569, AA13

Roederer I. U., Lawler J. E., Sneden C., Cowan J. J., Sobeck J. S., Pilachowski C. A., 2008, *ApJ*, 675, 723

Sales L. V., et al., 2009, *MNRAS*, 400, L61

Siebert, A., Williams, M. E. K., Siviero, A., et al. 2011, *AJ*, 141, 187

Silk, J., & Bouwens, R. 2001, *NAR*, 45, 337

Simmons G. J., & Blackwell D. E., 1982, *A&A*, 112, 209

Snaith, O. N., Haywood, M., Di Matteo, P., et al. 2014, *ApJ*, 781, LL31

Sneden C., Lawler J. E., Cowan J. J., Ivans I. I., Den Hartog E. A., 2009, *ApJS*, 182, 80

Soubiran, C., & Girard, P. 2005, *A&A*, 438, 139

Stanford, L. M., & Lambert, D. L. 2012, *MNRAS*, 424, 2118

Steinmetz, M., Zwitter, T., Siebert, A., et al. 2006, *AJ*, 132, 1645

Stonkutė E., Tautvaišienė G., Nordström B., Ženovienė R., 2012, *A&A*, 541, A157

Stonkutė E., Tautvaišienė G., Nordström B., Ženovienė R., 2013, *A&A*, 555, A6

Trevisan M., Barbuy B., Eriksson K., Gustafsson B., Grenon M., Pompéia L., 2011, *A&A*, 535, A42

Unsöld A., 1955, *Physik der Stern Atmosphären*. Springer–Verlag, Berlin

Villalobos Á., Helmi A., 2009, *MNRAS*, 399, 166

Wilson M. L., et al., 2011, *MNRAS*, 413, 2235

Wyse, R. F. G., Gilmore, G., Norris, J. E., et al. 2006, *ApJ*, 639, L13

Yanny, B., Rockosi, C., Newberg, H. J., et al. 2009, *AJ*, 137, 4377

Zhang H. W., Zhao G., 2006, *A&A*, 449, 127

Zwitter, T., Siebert, A., Munari, U., et al. 2008, *AJ*, 136, 421

Santrauka

Naudodamiesi Nordström ir kt. (2004) Ženevos-Kopenhagos apžvalgos (ŽKA) katalogu, Helmi ir kt. (2006) identifikavo tris naujas koherentes žvaigždžių grupes, kurios pasižymi išskirtiniais kinematiniais parametrais. Helmi ir kt. teigimu, šios grupės yra įsiliejusios į mūsų Galaktiką palydovinių galaktikų liekanos.

Šiame disertacijos darbe iš aukštos skiriamosios gebos spektrų buvo tiriama dviejų iš Helmi ir kt. identifikuotų kinematinų grupių žvaigždžių detali cheminė sudėtis. Buvo siekiama išsiaiškinti, ar ŽKA kinematinų grupių žvaigždės skiriasi nuo Galaktikos disko bei kitų kinematinų srautų Saulės aplinkoje žvaigždžių, ar identifikuotosios grupės yra homogeniškos, ar iš tiesų šių ŽKA kinematinų žvaigždžių grupių kilmė yra užgalaktinė.

Nustatėme 37 1-osios ŽKA kinematinės grupės, 32 2-osios grupės, 15 palyginamųjų Galaktikos plonojo disko bei 5 palyginamųjų Galaktikos storojo disko žvaigždžių atmosferų pagrindinius parametrus (efektingą temperatūrą, gravitacijos pagreitį žvaigždės paviršiuje, metalingumą bei mikroturbulencijos greitį) bei 21 cheminio elemento gausas.

Kinematinų grupių žvaigždžių deguonies, α -elementų ir elementų, daugiausia pagaminamų r -procesu, gausos yra padidėjusios lyginant su plonuoju Galaktikos disku ir yra panašios į Galaktikos storojo disko žvaigždžių atmosferų cheminę sudėtį. Geležies grupės elementų ir elementų, daugiausia pagaminamų s -procesu, gausos sutampa su Galaktikos plonojo disko žvaigždžių atmosferų chemine sudėtimi bei cheminės evoliucijos modeliais.

Naudojant HR diagramas nustatėme, kad dauguma 1-osios ir 2-osios ŽKA grupių žvaigždžių priklauso dviems 8 ir 12 mlrd. m. amžiaus populiacijoms. Be to 2-osios grupės žvaigždžių amžius buvo patikslintas naudojantis Bajeso metodais.

ŽKA kinematinų grupių ir keleto kitų kinematinų srautų žvaigždžių cheminės sudėties ir kinematinų savybių palyginimas rodo, kad ŽKA grupių kilmė skiriasi nuo Galaktikos srautų, kurie, manoma, susidarė dėl dinaminio Galaktikos skersės poveikio.

Panaši cheminė tirtų ŽKA kinematinų grupių bei storojo Galaktikos disko su-

dėtis rodo, kad kinematinų žvaigždžių grupių ir storjo Galaktikos disko žvaigždžių formavimosi scenarijai yra galimai susiję.

Visų trijų ŽKA kinematinų grupių žvaigždžių atmosferų cheminė sudėtis, kinematika ir amžiaus pasiskirstymas palaiko scenarijų, kuriame Paukščių Tako galaktika evoliucijos pradžioje susijungė su praturtinta dujomis nykštukinė galaktika. Gali būti, kad visos trys ŽKA grupės susiformavo to paties įsiliejimo įvykio metu.

Renata Ženovienė

Curriculum Vitae

Date and place of birth: 13 March 1980, Lithuania

E-mail: renata.zenoviene@tfai.vu.lt

Education:

B.Sc. in Physics at Lithuanian University of Educational Sciences, 2008.

M.Sc. in Physics at Lithuanian University of Educational Sciences, 2010.

Ph.D. studies in Physical Science, Physics (02 P) at Institute of Theoretical Physics and Astronomy of Vilnius University, 2010 – 2014.

Professional improvement:

Engineer at Institute of Theoretical Physics and Astronomy of Vilnius University, 2009 – 2012.

Junior Researcher at Institute of Theoretical Physics and Astronomy of Vilnius University, 2012 – to present.

Erasmus practice at Nordic Optical Telescope, La Palma, Spain, July 2011 – September 2011.

Observing Experience:

Optical High Res. Spectroscopy (Nordic Optical Telescope).